Constraining Long-Term NO$_x$ Emissions over the United States and Europe using Nitrate Wet Deposition Monitoring Networks

Amy Christiansen[1,3], Loretta J. Mickley[2], Lu Hu[3]

[1]Division of Energy, Matter & Systems, University of Missouri – Kansas City, Kansas City, MO, 64114, USA
[2]John A. Paulson School of Engineering and Applied Sciences, Harvard University, Cambridge, MA, 02138, USA
[3] Department of Chemistry and Biochemistry, University of Montana, Missoula, MT, 59812, USA

Correspondence to: Amy Christiansen (achristiansen@umkc.edu)

Abstract. Nitrogen oxides (NO$_x$ = NO + NO$_2$) play a critical role in regulating tropospheric chemistry, yet NO$_x$ emission estimates are subject to large uncertainties, casting doubt on our ability to accurately model secondary pollutants such as ozone. Bottom-up emissions inventories are subject to a number of uncertainties related to estimates of emission activities, scaling factors, and fuel sources. Here, we provide an additional constraint on NO$_x$ emissions and trends using nitrate wet deposition (NWD) fluxes from the United States National Atmospheric Deposition Program (NADP) and the European Monitoring and Evaluation Programme (EMEP). We use these NWD measurements to evaluate anthropogenic and total NO$_x$ trends and magnitudes in the global Community Emissions Data System (CEDS) emissions inventory and the GEOS-Chem chemical transport model from 1980-2020. Over both the United States and Europe, observed NWD trends track well with anthropogenic NO$_x$ emissions from the CEDS inventory until 2010, after which NWD trends level out in contrast to continued decreases in CEDS. After 2010, NWD trends are able to reproduce total NO$_x$ emissions trends when the influences of both anthropogenic and background sources are considered. Observed NWD fluxes are also able to capture NO$_x$ emissions decreases over the 2020 COVID-19 lockdown period and are consistent with satellite and surface measurements of NO$_2$. These results suggest that NWD fluxes constrain total NO$_x$ emissions well, whether trends are driven by anthropogenic or background sources. We further compare modelled and observed NWD to provide an additional line of evidence for potential overestimates of anthropogenic NO$_x$ in emissions inventories. Over the United States, we find that NWD is overestimated in summer from 1980-2017 by 15-20% on average (interquartile range: 11-31%), with overestimates most prominent in the eastern US after 2000 (20% on average), implying an overestimate of NO$_x$ emissions in the CEDS inventory (0.5x0.5-degree resolution). Over Europe, we find that modeled NWD is overestimated in all seasons from 1980-2017, with the strongest average overestimates occurring in summer and fall (175% and 170%, respectively). These overestimates may be reduced by cutting anthropogenic NO$_x$ emissions by 50% in CEDS over Europe (i.e., cutting the 1980-2017 average annual emissions from 2.6 to 1.3 Tg N), but summertime and fall NO$_x$ may still need to be reduced further for observations and models to align. Overestimates may extend to other inventories such as the EMEP inventory, which estimates comparable but lower emissions than CEDS, with a 1990-2017 average of 2.1 Tg N relative to the CEDS 1990-2017 average of 2.4 Tg N. We find that NO$_x$ emission reductions over Europe improve model ozone at the surface, reducing the model summertime ozone overestimate from 14% to 2%.

1 Introduction

Nitrogen oxides (NO_x), the sum of nitric oxide (NO) and nitrogen dioxide (NO_2), play a critical role in regulating ozone, aerosol, and hydroxyl radical levels in the troposphere (Monks et al., 2009; Murray et al., 2013; Hu et al., 2017). Direct exposure to NO_x is linked to increased instances of childhood asthma (Takenoue et al., 2012; Gauderman et al., 2005). Health impacts of the photochemical products of NO_x, such as ozone and particulate matter, include respiratory illness, cardiovascular disease, and premature mortality (Burnett et al., 2014; Pope et al., 2015; Turner et al., 2011; Monks et al., 2015; Bell et al., 2006). At the surface, NO_x has a short lifetime of 4-21 hours depending on season (Shah et al., 2019; Liu et al., 2016; Laughner and Cohen, 2019) and is rapidly oxidized to higher oxides such as peroxy nitrates (RO_2NO_2), alkyl nitrates ($RONO_2$), and nitric acid (HNO_3), which are typically removed via deposition (Kenagy et al., 2018). Recent observations have shown increases in NO_x lifetimes of a few hours since 2006 (Laughner and Cohen, 2019), which may increase the distance NO_x travels before it eventually deposits. However, the small increase in lifetimes is not expected to substantially impact wet deposition since deposition processes such as rainout occur on longer timescales (e.g., days). This suggests that NWD measurements can be used over long timeframes to track NO_x emissions trends, despite potential changes in NO_x lifetime over decades. Nitric acid deposits as acid rain and negatively impacts plant and wildlife health (Singh and Agrawal, 2008). Anthropogenic fossil fuel combustion contributes to a majority of total NO_x emissions, while natural processes such as biomass burning, soil microbial activities, and lightning are important sources for certain seasons and regions. Anthropogenic NO_x emissions have shifted rapidly in the past few decades due to emissions control regulations, technological innovations, and economic development (Lamsal et al., 2011; Duncan et al., 2016; Krotkov et al., 2016; Barkley et al., 2017; Miyazaki et al., 2017; Jiang et al., 2018).
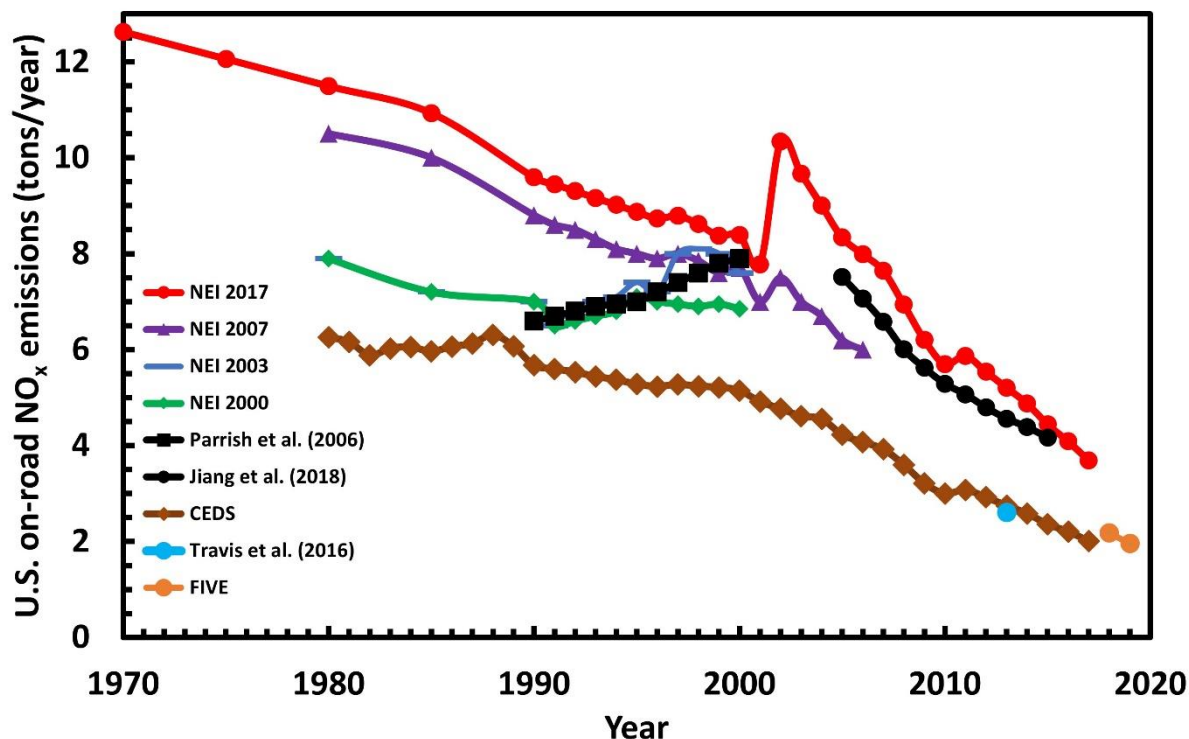
Bottom-up NO_x emissions estimates are subject to many uncertainties, hindering the accurate estimation of NO_x emissions in inventories commonly used in atmospheric chemistry models and thus representation of secondary products such as ozone and particulate matter. Bottom-up inventories are typically calculated by accounting for all activities that generate emissions, then applying measurement- or model-based emissions factors to those activities. Emission factors of anthropogenic sources depend on fuel type, technology, and combustion condition. In addition, natural sources of NO_x are also difficult to quantify in part due to their sporadic nature. Top-down studies based on urban or near-source NO_x emissions suggest that mobile emissions are overestimated in many emissions inventories (McDonald et al., 2013; Anderson et al., 2014; Canty et al., 2015; Goldberg et al., 2016; McDonald et al., 2018; Kota et al., 2014). For example, NO_x emissions from the United States (US) Environmental Protection Agency (EPA) National Emissions Inventory (NEI) must be reduced by 30-60% in order to reconcile models with aircraft observations of NO_x and ozone in the southeast US during summer 2013 (Travis et al., 2016; McDonald et al., 2018). Most top-down studies have attributed model-observation disagreements to emissions errors from mobile sources, as power

plant emissions in the US are considered to be better known due to regulatory continuous emission monitoring systems (CEMS)

65   that report hourly averaged emissions (Frost et al., 2006; Peischl et al., 2010). On an annual basis, total mobile emissions from diesel engines generally agree well with NEI estimates (Dallmann and Harley, 2010), but the source contributions to these totals do not agree. Dallman and Harley (2010) found that on-road diesel emissions may be underestimated in the NEI 2005, indicating uncertainty in source sectors and emissions factors. However, other analyses performed during wintertime showed good agreement between aircraft measurements and both the NEI 2011 and NEI 2014 (Salmon et al., 2018; Jaeglé et al., 2018).

70

Figure 1 shows estimates of on-road mobile emissions from various emissions inventories and inferred emissions from ground, aircraft, and satellite-based observations (Jiang et al., 2018; Travis et al., 2016; Parrish, 2006), providing a further illustration of the wide range of NO_x emissions estimates within and between inventories and measurements. Magnitudes do not agree across different estimates, even amongst the EPA NEI from different years, although it should be noted that methods for

75   calculating NEI estimates change from year to year (e.g., NEI 2003 vs. NEI 2007 vs. NEI 2017), and previous NEI version estimates are not changed to reflect these updates. For example, the most recent NEI (2017) used an updated version of the Motor Vehicle Emissions Simulator (MOVES) model, increasing nonroad NO_x emissions estimates from previous NEIs. While NEI versions are not meant to be used as a time series, the large changes in NO_x magnitudes between NEI versions brought about by updated methods illustrate the uncertainty inherent in NO_x emissions inventories. Emissions inventories show similar

80   trends after 2005 but differ greatly in trends prior to 2005 (Fig. S1). Disagreement in magnitudes and trends amongst a wide variety of bottom-up and top-down emissions inventories occur in many regions around the world and highlight the uncertainty in current NO_x emissions estimates (Elguindi et al., 2020).

U.S on-road vehicle NO$_x$ emission estimates

Recent studies have shown discrepancies in NO$_x$ trends between bottom-up emissions inventories and observational constraints (Jiang et al., 2018; Silvern et al., 2019; Elguindi et al., 2020). For example, Jiang et al. (2018) and Silvern et al. (2019) noted

95   a slowdown in the decrease of NO$_x$ emissions over the US after 2010 in satellite NO$_2$ and ground-based nitrate wet deposition (NWD) measurements that was not represented in the NEI. In this post-2010 period, NEI NO$_x$ emissions continued to decrease steadily, while both satellite and NWD measurements leveled off. Silvern et al. (2019) suggested that this leveling off of NO$_x$ emissions trends was due to anthropogenic emissions becoming less prominent in recent years, allowing relatively steady background NO$_x$ emissions (e.g., lightning, soils, etc.) to play a larger role in determining total NO$_x$ trends. More recently, He

100   et al. (2022) applied a deep learning model to investigate drivers of observed NO$_x$ trends and confirmed that satellite NO$_2$ measurements were more representative of background sources, leading to a slowdown in NO$_x$ decreases. This idea will be explored in-depth in this work in Sects. 3.1 and 3.2.

4

Traditional top-down evaluations of emissions inventories often use surface monitoring networks, aircraft campaigns, and satellite measurements as constraints (Anderson et al., 2014; Brioude et al., 2013; Canty et al., 2015; Castellanos et al., 2011; Jaeglé et al., 2018; Jiang et al., 2018; Lamsal et al., 2011; Oner and Kaynak, 2016; Salmon et al., 2018; Souri et al., 2016; Szymankiewicz et al., 2021; Goldberg et al., 2019), yet these methods contain limitations. Ground-based NO_2 monitoring stations are primarily located in urban areas that mostly reflect local emissions due to the short lifetime of NO_2, and thus they are not representative of an entire region. Aircraft campaigns collect intensive measurements during a short period, but only offer information for a few snapshots in the weeks they are conducted. Daily satellite retrievals improve on spatial and temporal limitations of aircraft and surface measurements, but these measurements are more sensitive to free tropospheric than boundary layer NO_2 by a factor of 3-4 (Martin, 2002; Krotkov et al., 2017), confounding satellite-derived trends for near-surface NO_x. Further, satellite-derived NO_2 columns rely on air mass factors calculated from atmospheric models which employ *a priori* estimates of gas vertical profiles. These profiles also contain errors in their representation of transport and chemical processes (Elguindi et al., 2020; Jiang et al., 2013; Stavrakou et al., 2013), which can stem from uncertainties in the observations used to constrain the models. Current low-orbital satellites also detect at only one time point every day or every few days. As NO_x emissions show strong diurnal patterns and changes with planetary boundary layer height, these single time point observations may not be fully representative of emissions.

Long-term, regular measurements of NWD located in non-urban areas provide another independent and often overlooked constraint on NO_x emissions that is sensitive to anthropogenic and background sources of NO_x. NO_x is quickly oxidized to form nitric acid gas and nitrate aerosol, both of which are scavenged efficiently by precipitation. The magnitude of nitrate deposited via precipitation is related to total NO_x emissions due to the short lifetime of NO_x (Silvern et al., 2019). Most NO_x is derived from combustion processes, and thus NWD is closely related to anthropogenic sources (Butler et al., 2003; Galloway et al., 2003; Du et al., 2014; Paulot et al., 2014; Sickles II and Shadwick, 2015; Li et al., 2016). Background sources of NO_x, such as soils and lightning, also contribute substantially to NWD (Zhang et al., 2012). Both the US National Atmospheric Deposition Program (NADP) and the European Monitoring and Evaluation Programme (EMEP) have been monitoring atmospheric composition, including precipitation chemistry, since the 1970s, providing a long-term, independent network of observations that can be related to NO_x emissions (Tørseth et al., 2012; Lamb and Bowersox, 2000). Both networks are designed for sampling regionally representative background air and precipitation chemistry with high quality control procedures (Tørseth et al., 2012; Lamb and Bowersox, 2000).

Here, we use long-term measurements of NWD to constrain NO_x emissions from 1980-2020 over the US and Europe. We calculate NWD for each measurement site and use these observed NWD fluxes to assess NO_x emissions from a commonly used global anthropogenic emission inventory (the Community Emissions Data System; CEDS) for potential biases in trends. To determine drivers of NWD trends and test the sensitivity of NWD to changes in NO_x emissions, we perform a series of

5

sensitivity tests in the 3D chemical transport model GEOS-Chem and analyze the observed sensitivity of NWD to urban NO_x emission reductions during COVID-19 lockdowns in spring 2020. We also compare modelled and measured NWD to assess potential biases in NO_x emissions magnitudes. Finally, we investigate the impact of NWD-constrained anthropogenic NO_x

140   emissions on tropospheric and surface ozone.

2 Methods

2.1 Observations

For the contiguous United States (CONUS) domain, long-term monthly average measurements of NWD were downloaded

145   from the NADP website (https://nadp.slh.wisc.edu/networks/national-trends-network/) (Lamb and Bowersox, 2000), and nitrate deposition was calculated in kg N ha^{-1}. The NADP configures each site in its network with an automated precipitation collector and a rain gauge, and composite samples are collected year-round and analyzed on a weekly basis. All samples are analyzed at the Central Analytical Laboratory (CAL) at the Wisconsin State Laboratory of Hygiene in Madison, WI, USA for a variety of ions, acidity, and conductance. Ion concentrations are measured via ion chromatography. The network performs

150   quality assurance for data completeness and accuracy before making it publicly available, and previous analyses have found good agreement (<7% difference) between the network and co-located independent nitrate ion measurements (Nilles et al., 1994; Lamb and Comrie, 1993). In our analysis, we use data from 156 NADP sites that have at least 32 years of data from 1980-2020 and at least 80% of valid monthly measurements (Fig. 2). Sites are located primarily in rural areas away from point sources of pollution.

155

Monthly mean NWD measurements for the European domain were provided by EMEP, the data from which is compiled and made available by the Norwegian Institute for Air Research (NILU) (https://ebas.nilu.no/data-access/) (Tørseth et al., 2012). Measurement data is compiled from many countries on a year-round basis. Daily precipitation samples are collected via automatic collectors and analyzed by laboratories weekly via ion chromatography, similar to the protocols used by the NADP.

160   To quantify the accuracy and precision of the samples, internal checks are performed by comparing samples against known concentrations, and external checks are occasionally implemented. Evaluation of nitrate ion measurements during laboratory inter-comparisons shows good agreement with each other and expected values (Tørseth et al., 2012). Only valid, non-contaminated samples are used in the calculation of monthly mean concentrations. In our analysis, we ensure all data has at least 28 years from 1980-2020 and at least 70% of valid monthly measurements. These data requirements are relaxed from

165   those for NADP due to the smaller size of this network. We find only 28 sites that meet these requirements (Fig. 2). Similar to NADP, most sites are located in areas that are considered representative of the air mass (avoiding inversion areas and mountaintops) away from sources of pollution including point, road, and agricultural sources. All samplers are required to be

placed >1 km away from gravel roads, farmyards, and tilled agricultural fields to limit the impact of dust particles (Tørseth et al., 2012).

170

We do not consider dry deposition in this analysis due to observational limits. Dry deposition measurements are available only after 2000 over the CONUS from the Clean Air Status and Trends Network (CASTNET), and there are only four sites over Europe (EMEP) with analysis timeframes long enough to include. There are also many uncertainties with regard to both observations and model representation of dry deposition. Estimates of dry deposition velocities must be made to determine dry

175 deposition fluxes at observation sites. This is typically done by using a multi-layer model (Finkelstein et al., 2000; Meyers et al., 1998), which calculates deposition velocity as a function of chemical composition, meteorology, and vegetation. Limitations to this method include the lack of meteorological measurements co-located with observation sites, requiring the use of a chemical transport model to estimate deposition velocities. These velocities are uncertain, and different velocity estimation methods can result in fluxes that differ by ~1.6x (Schwede and Lear, 2014). A recent study also shows a high bias

180 in GEOS-Chem for nitrate dry deposition that persists throughout seasons and across multidecadal timeframes (Dutta and Heald, 2023), largely due to a model overestimate of dry deposition velocity of HNO_3. The uncertainty inherent to the dry deposition observations, the limitations of the observations, and the known bias in GEOS-Chem makes dry deposition a more uncertain comparator for NO_x trends than wet deposition. Excluding dry deposition may lead to some bias in capturing anthropogenic trends, as dry deposition tends to be more influenced by urban sources, but seasonal variations, annual trends,

185 and geographic distributions are similar to those found in wet deposition (Dutta and Heald, 2023).
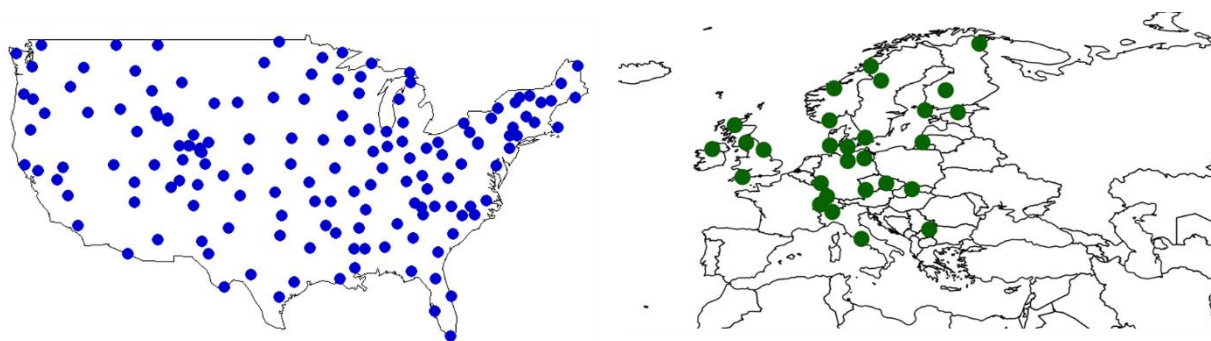

Figure 2. Location of NADP (left) and EMEP (right) long-term monitoring sites for nitrate wet deposition measurements used in this study. See the text for data selection criteria.

190

Surface ozone data from 1990-2014 were obtained from the Tropospheric Ozone Assessment Report (TOAR) Surface Ozone Database (Schultz et al., 2017), which has been compiled and processed by the TOAR Database team and made public via https://doi.org/10.1594/PANGAEA.876108. We obtain monthly aggregates from sites over Europe that have at least 70% of all hourly ozone measurements available for each year. The following criteria were followed to ensure consistent data for the

long timeframe: 1) at least 2 monthly observations per season, 2) at least 8 monthly observations per year, and 3) at least 15 years of data (Christiansen et al., 2022). The 186 TOAR site locations are shown in Figure S2. All sites are classified as "rural," which is defined as: 1) NO_2 column $\leq 8x10^{15}$ molecules cm^{-2} as measured by the Ozone Monitoring Instrument (OMI), 2) an averaged nighttime light intensity index of ≤ 25 within a 5 km radius of the site, and 3) a maximum population density of $\leq$ 3000 people km^{-2} within a 5 km radius of the site (Schultz et al., 2017). Additionally, only daytime ozone data is used, which is defined as measurements between 8 and 20 hours local time. The surface site locations are summarized in Figure S2.

Ozone observations above the surface were provided by ozonesonde vertical profile measurements. Individual vertical profiles from 1990-2017 were downloaded from the World Ozone and Ultraviolet Data Center (WOUDC) (https://woudc.org/data/explore.php) and the Harmonization and Evaluation of Ground-based Instruments for Free Tropospheric Ozone Measurements (HEGIFTOM) working group of the Tropospheric Ozone Assessment Report, Phase II (TOAR-II) (https://hegiftom.meteo.be/datasets/ozonesondes). The most updated information available at each site was used. The ozonesonde community is currently reprocessing and homogenizing data to account for changes in ozonesonde preparation and procedures with the goal to reduce measurement biases associated with these changes (Tarasick et al., 2016; Van Malderen et al., 2016; Witte et al., 2018; Sterling et al., 2018; Ancellet et al., 2022). Over Europe, these homogenization efforts impact 3 of the 7 ozonesonde sites (De Bilt, Hohenpeissenberg, and Uccle). It should be noted that, since the site Payerne has homogenized data for only part of the timeframe, we use the non-homogenized data in this analysis to remain consistent throughout. Following our previous work in Christiansen et al. (2022), we apply these data completion requirements for inclusion in the analysis: 1) at least 3 observations per month, 2) at least 2 monthly observations per season, 3) at least 8 monthly observations per year, and 4) at least 16 years of data. The ozonesonde site locations are summarized in Figure S2.

2.2 Model Simulations

We used multiple simulations of GEOS-Chem version 12.9.3 (GC) (Bey et al., 2001) at different horizontal resolutions (GC 4°x5° (latitude x longitude) and GC 2°x2.5°; DOI: 10.5281/zenodo.3974569) in this analysis, summarized here and in Table 1. We primarily show results from the GC 2°x2.5° simulation but used GC 4°x5° for sensitivity simulations due to computational constraints. These simulations were performed using the native 72 vertical pressure levels from 1980-2017 and were driven by reanalysis data from the Modern-Era Retrospective analysis for Research and Applications version 2 (MERRA-2) (Gelaro et al., 2017) developed by the NASA Global Modeling and Assimilation Office (GMAO). GEOS-Chem includes detailed HO_x-NO_x-VOC-ozone-BrO_x-aerosol tropospheric chemistry with over 200 species, and this version includes updated halogen (Wang et al., 2019) and isoprene chemistry (Bates and Jacob, 2019). Emissions were computed by the Harvard-NASA Emissions Component (HEMCO) (Keller et al., 2014). We used the Community Emissions Data System (CEDS) for global anthropogenic emissions at a monthly 0.5°x0.5° resolution (Hoesly et al., 2018; McDuffie et al., 2020). Model simulations

were carried out only until 2017 because the anthropogenic emissions from CEDS were available only until 2017 at the time. Biogenic VOC emissions were calculated at each emissions timestep (every 30 minutes at 2°x2.5°) by the Model of Emissions of Gases and Aerosols from Nature version 2.1 (MEGAN) with meteorological inputs from MERRA-2 (Guenther et al., 2012)

230 as implemented by Hu et al (2015). Biomass burning emissions were provided by the Global Fire Emissions Database (GFED) version 4s for 1997 and onward (Giglio et al., 2013) at a monthly resolution. Prior to 1997, biomass burning emissions were estimated using a GFED4s climatology with interannual variability imposed using scale factors from the Total Ozone Mapping Spectrometer (TOMS) aerosol index (Duncan, 2003). Biogenic soil NO_x emissions were calculated online (Hudman et al., 2012). Lightning NO_x emissions were constrained at ~6 Tg N per year to match satellite observations (Martin et al., 2007) and

235 distributed to match satellite climatological observations of lightning flashes while maintaining coupling to deep convection from meteorological fields (Murray et al., 2012). Monthly mean methane concentrations were prescribed in the model surface layer from interpolation of the long term NOAA ESRL GMD flask observations (Murray, 2016). Model wet deposition is described by Liu et al. (2001) for water-soluble aerosols and by Amos et al. (2012) for gases. For comparison to observations, model monthly averages of NWD, calculated as kg N ha^{-1}, were sampled at the locations of each network site throughout the

240 US and European domains. For simplicity, we refer to the GC 2°x2.5° simulation as GC throughout this work.

Table 1. Description of GEOS-Chem simulations used in this study.

Model	GEOS-Chem version 12 (4°x5° and 2°x2.5° resolution)
Horizontal resolution (latitude x longitude)	4°x5° and 2°x2.5°
Chemistry	v12.9.3[a]
Meteorology	Modern-Era Retrospective analysis for Research and Applications version 2 (MERRA-2)
Anthropogenic Emissions	Community Emissions Data System (CEDS)[b]
Biomass burning Emissions	Global Fire Emissions Database version 4s (GFED4s)[c]
Biogenic VOC Emissions	Model of Emissions of Gases and Aerosols from Nature version 2.1 (MEGAN)[d]

[a]DOI: 10.5281/zenodo.3974569

[b]Hoesly et al. (2018); CEDS provides monthly average anthropogenic emissions at the 0.5°x0.5° resolution using previously

245 existing emissions inventories.

[c]Giglio et al. (2013) after 1997; prior to 1997, estimated using a GFED4s climatology with interannual variability imposed using scale factors from the Total Ozone Mapping Spectrometer aerosol index as in Duncan et al. (2003); monthly 0.25° resolution.

[d]MEGANv2.1 from Guenther et al. (2012) as implemented by Hu et al (2015). Biogenic VOC emissions are calculated online depending on the emissions timestep (e.g., hourly at 4°x5°, every 30 minutes for 2°x2.5° resolution).

We also performed four sensitivity simulations for 1980-2017 at 4°x5° resolution: constant anthropogenic emissions but varying meteorological fields ('Meteorology'), constant meteorology with varying anthropogenic emission inputs ('Emissions'), halved anthropogenic NO_x emissions over Europe ('Half-NO_x'), and no global biomass burning emissions ('No-Fires'). Here, the Meteorology simulation cycled only anthropogenic emissions at constant 1980 values while allowing meteorology to proceed normally, so that trends in the simulation were primarily due to the effects of changing meteorological factors. Similarly, the Emissions simulation cycled meteorological inputs at constant 1980 values, but emissions were allowed to evolve normally. The Half-NO_x simulation was performed the same as the base simulation, but anthropogenic NO_x emissions from the CEDS inventory were halved over Europe to investigate the impact on NWD, which is discussed in more detail in Sect. 3.4. Finally, in the No-Fires simulation, all emissions evolved normally except for biomass burning emissions, which were set to zero. These sensitivities allowed for the exploration of drivers of NWD trends, as well as the sensitivity of NWD to changes in NO_x emissions.

To complement the simulations described above, we also used a simulation from a previous version of GEOS-Chem (version 10-01) at 4°x5° resolution from 1980-2010 as described by Hu et al. (2017). Differences relevant to our analysis, summarized in Christiansen et al (2022), include 1) the MERRA reanalysis meteorological data (Rienecker et al., 2011), 2) 47 vertical pressure levels, 3) global anthropogenic and biomass burning emissions from the MACCity inventory, and 4) a coarser horizontal resolution. In the MACCity inventory, anthropogenic emissions are provided at a decadal resolution and interpolated to an annual basis, and monthly biomass burning emissions are provided by the MACCity inventory prior to 2005 and based on the Representative Concentration Pathway (RCP) 8.5 emissions scenario after 2005 (Granier et al., 2011). The 1980-2010 timeframe was chosen for the model because of the limited availability of MERRA meteorology fields at the time the run was performed. Including this simulation provides a point of comparison to our GC simulations. We use this to show that the discrepancies between modelled and observed NWD are not unique to a specific model version. Instead, we show that these discrepancies are consistent between model versions that use different settings, different emissions inventories, and contain different chemistry updates. This allows us to assess whether model-observations discrepancies in NWD are due to internal model processes or emissions inventories.

In all models, we corrected for potential precipitation biases, as model errors in precipitation propagate to NWD. We corrected for these potential biases using independent, high-resolution observations which have been interpolated to a grid. We use the Parameter-elevation Relationships on Independent Slopes Model (PRISM) at 4-km grid cell resolution over the US and E-OBS over Europe (Daly et al., 2008; Haylock et al., 2008) at 0.25° grid cell resolution, which we sampled at the location of

each network site. The precipitation correction is shown below in Eq. (1), which has been applied previously for analyses of wet deposition fluxes (Liu et al., 2021; Paulot et al., 2014; Silvern et al., 2019):

$$Corrected\ NWD = Model\ NWD\ *\frac{p_{obs}}{p_{mod}} \tag{1}$$

285 Here, p represents the amount of precipitation in each month from PRISM or E-OBS within the grid cell containing the NWD sites and the model output. All data analysis was performed using R statistical software (R Core Team, 2013).

3 Results and Discussion

3.1 Observational Trends

290
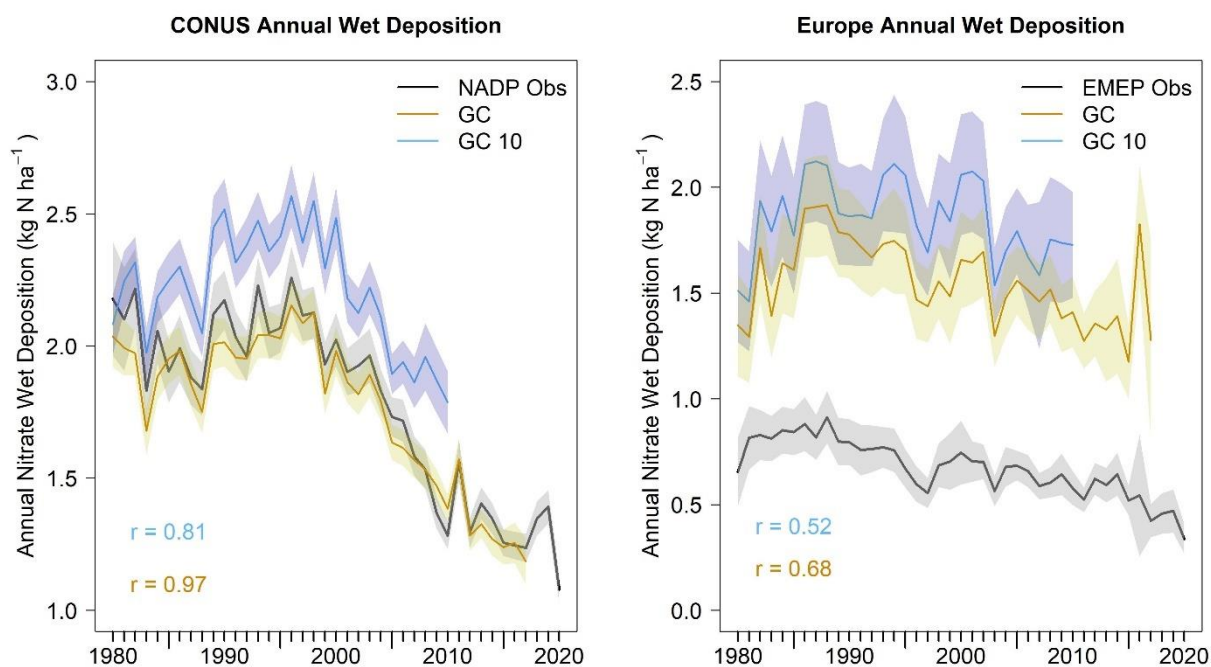
Figure 3. Observed and modeled nitrate wet deposition (NWD) from 1980 to 2020, including the 2020 COVID lockdown period, averaged over the contiguous United States (CONUS) and Europe, in units of kg N ha^{-1}. Shown are annually-averaged monthly mean observations (black) and base simulation results (gold) from GEOS-Chem (GC) at 2°x2.5° resolution. Results from an earlier model version at different resolution (GC v10-01, 4°x5°) are shown in blue for 1980 to 2010. The shaded regions represent one standard
295 **deviation of the monthly mean NWD. Correlation coefficients for each simulation with observations are shown inset. The 2016 jump in NWD concentrations in GC in Europe is due to a spike in precipitation during that year in the E-OBS dataset (Fig. S3).**

We find that over the CONUS, the strongest decreases in NWD occur from 2000-2010 and average -4.1 ± 1.2%/yr (mean ± standard deviation). NO_2 measurements are commonly used to infer NO_x concentrations due to the short lifetime of NO_2,

11

300   which results in robust correlations between NO_x emissions and NO_2 column amounts (Goldberg et al., 2021). Prior to 2010, there is generally good agreement between NWD and measurements of NO_2 from surface stations and satellites when analyzed on a regional scale. The EPA's Air Quality System (AQS) surface NO_2 trends decrease by -6.6 ± 1.4 %/yr from 2005-2009 and satellite NO_2 trends decrease by -6 ± 0.5%/yr (Silvern et al., 2019), both of which are in good agreement with NWD measurements over that timeframe (-5.7 ± 1.9%/yr). It should be noted NWD is most useful as a constraint on regional spatial

305   scales, as NWD observations are located in rural areas influenced by transport and background emissions, which can show different trends from urban areas (Silvern et al, 2019).

Over Europe, decreases in NWD are evident since the late 1980s, but occur most strongly since the 2000s and are in good agreement with satellite and surface NO_2 measurements. We calculate a 1980-2017 decrease in NWD over Europe of 19 ±

310   10%, similar to the 23% calculated by Tørseth et al. (2012) for 1990-2009. Trends in assimilated satellite NO_2 measurements over western Europe show an average decrease of -0.9%/yr from 2005-2014 (Miyazaki et al., 2017), which agrees with the decrease in western Europe NWD measurements over that same timeframe (-0.9% ± 2.6%/yr).

After 2010 over the CONUS, decreases in NWD observations slow down, averaging -1.2 ± 2.9%/yr from 2011-2019. This

315   slowdown in trends is consistent with satellite measurements of NO_2, which also record a flattening of the trend from 2011-2015 at -1.7%/yr (Jiang et al., 2018). This slowdown has been attributed to the increasing sensitivity of satellite measurements to free tropospheric NO_2, which in recent years has contributed an increasingly larger portion of column NO_2 as emissions of anthropogenic NO_x have declined (Silvern et al., 2019). Consistent with this hypothesis, NWD and satellite NO_2 trends over the CONUS do not agree with surface AQS NO_2 measurements, which have decreased by -4.5%/yr since 2010 (Silvern et al.,

320   2019); the CEDS inventory also shows strong decreases after 2010, averaging -4.3 ± 0.6%/yr (Fig. S4). Over Europe, although NWD trends are noisier due to a smaller number of sites compared to the CONUS, we also find a leveling off of trends since 2010. NWD trends level off from -1.9 ± 2.2%/yr from 2000 to 2010 to -1.4 ± 3.6%/yr from 2010-2019. Again, this is in contrast with the CEDS inventory (Fig. S4), which shows a ~2 times faster decrease (an average decrease of -4.0 ± 0.9%/yr) since 2010.

325

This discrepancy in trends between NWD, satellite NO_2 measurements, surface NO_2 concentrations, and anthropogenic NO_x emissions has been noted previously and can be explained by a change in the relative importance of emissions sources in driving NO_x trends. In CEDS and GEOS-Chem, prior to 2010, anthropogenic NO_x made up 79% of total NO_x emissions in the CONUS and 88% in Europe, but anthropogenic emissions have decreased rapidly since the 1980s in both regions. In contrast,

330   the magnitude of lightning, soil, and biomass burning NO_x emissions have remained relatively steady over the past few decades; together they make up 34% of the total NO_x emissions profile in 2017 in the CONUS and 17% in Europe in GEOS-Chem (Fig. S5). Post-2010 trends in NO_x are therefore no longer primarily determined by anthropogenic emissions, and the flat trends of non-anthropogenic emissions now play a larger role in total trends. Since NWD sites are primarily rural and are

influenced by background NO_x emissions, we also observe a slowdown in NWD trends that reflects the increased importance of background NO_x emissions in determining trends. Our results support the findings in Silvern et al. (2019) and He et al. (2022) that background emissions such as soils and lightning play an increasingly important role in determining NO_x emissions trends in rural regions, as NO_x anthropogenic emissions rapidly decline over the US and Europe.

Observed trends in NWD also agree with satellite and surface-derived NO_2 trends during the COVID-19 lockdown period in March and April 2020, lending further evidence to the ability of NWD to capture large changes in NO_x emissions. Satellite measurements may be more influenced by urban emissions than NWD, but satellites are sensitive to background NO_2 similar to how NWD is sensitive to background NO_x, and trends between satellite NO_2 and NWD have been shown to match closely when averaged over a regional scale (Silvern et al., 2019). Despite the influence of background emissions, both NWD and satellite NO_2 observations capture large-scale changes in anthropogenic emissions (Fig. 3; pre-2010 trends). Figure 3 shows the decrease in NWD from 2019 to 2020 as measured across the NADP and EMEP networks. For the entire year of 2020, observations show a 22% decrease in NWD values over the CONUS and 28% over Europe. If we compare just March-April of 2019 to March-April of 2020, we find an average decrease of 37% in NWD values over the CONUS and 42% over Europe. These results are consistent with other analyses which estimate NO_x emissions decreases during COVID-19 lockdowns. Over the United States, satellite NO_2 total columns showed decreases over the lockdown period ranging from 20-40% (Bauwens et al., 2020; Qu et al., 2021). Over Europe, satellites measured decreases of 7-40% (Bar et al., 2021), with much of that decrease occurring over western Europe (20-30%) and at the surface (20-50%) (Bauwens et al., 2020). NO_x decreases during lockdowns are mostly associated with a reduction in vehicle traffic (Rossi et al., 2020; Baldasano, 2020; Kerr et al., 2021), and background sources of NO_x did not change considerably during this timeframe (Kerr et al., 2021). These results show that, despite becoming less sensitive to anthropogenic emission trends in the U.S. and Europe, NWD is still useful for constraining changes such as those resulting from COVID-19 lockdowns or energy usage shifts occurring in developing countries.

3.2 Model reproduction of trends

Trends and magnitudes in NWD are well-reproduced by GC over the CONUS (Fig. 3). During the largest decrease, 2000-2010, GC shows a significantly ($p<0.05$) decreasing trend of -3.4 ± 0.8%/yr, which agrees with significant observed decreases in NWD of -4.1 ± 1.2%/yr. NWD magnitudes predicted by GC typically fall within measurement uncertainty ranges (<3% difference) when aggregated over the entire US domain. GC v10-01 also shows a significant decrease of -2.7 ± 1.8%/yr for the same period. The post-2010 leveling off of the decreasing trend in NWD described earlier, also observed in satellite NO_2 measurements (Jiang et al., 2018), is captured by GC, suggesting that the CEDS NO_x trends are correct with the constraints provided by NWD observations.

Trends in observed NWD over Europe are captured fairly well by both simulations (R>0.5) (Fig. 3). Observed NWD trends are small throughout the timeframe, with observations showing only a change of -1.4 ± 0.8%/yr. GC shows an average decrease of -0.5 ± 1.0% throughout the timeframe, with large uncertainty due to increases at the beginning and end of the time series. If the timeframe is restricted to include the period of greatest decline, 1990-2015, GC shows a decrease of -1.2 ± 0.9%/yr, in

370   good agreement with the observed decrease of -1.4 ± 1.1%/yr over this time period. However, the GC v10-01 simulation (driven by MACCity) does not capture trends as well (i.e., -0.2 ± 1.2%/yr vs. observed -1.3 ± 0.9%/yr in 1980-2010; -0.8 ± 1.3%/yr vs. observed -1.1 ± 1.4%/yr in 1990-2010). We attribute this discrepancy largely to the lack of fine temporal resolution in MACCity anthropogenic emissions (decadal in MACCity vs monthly in CEDS). Despite the good agreement of trends over Europe in the newer GC version (driven by CEDS), our GC simulation predicts NWD fluxes that are on average 2.3 times

375   greater than observed NWD, and GC v10-01 predicts slightly higher NWD (2.6x). These findings suggest that CEDS and MACCity NO_x emissions over Europe are overestimated on a region-wide scale in GEOS-Chem, which will be explored further in Sect. 3.4.

Trends in GC-predicted NWD since 1980 are driven primarily by changes in anthropogenic emissions rather than

380   meteorological factors. Figure 4 shows the results of the three sensitivity simulations that demonstrate the role of anthropogenic emissions, fire emissions, and meteorology in simulated NWD trends. Over both the United States and Europe, the only simulation that does not follow the trendline of the base simulation is the Meteorology simulation. Trends for the Emissions and No Fires simulations are similar to the base simulation in both domains. As long as anthropogenic emissions are allowed to evolve over time, the trendline in NWD can be matched. Further, changes in precipitation are unlikely to be responsible for

385   the observed changes in NWD, as precipitation rates have remained relatively flat, or even increased, in opposition to NWD trends (Fig. S3). This, along with our sensitivity simulations, suggests that the changes in anthropogenic emissions of NO_x are most influential in driving overall NWD trends in GC. In sum, our findings suggest that the NWD mechanism within GC can capture observed NWD and that the NWD trend generated by GC is influenced most strongly by anthropogenic NO_x emissions. Next, we explore trends in total NO_x emissions in GEOS-Chem and anthropogenic NO_x emissions from the CEDS inventory,

390   focusing on differences in the period after 2010.

14
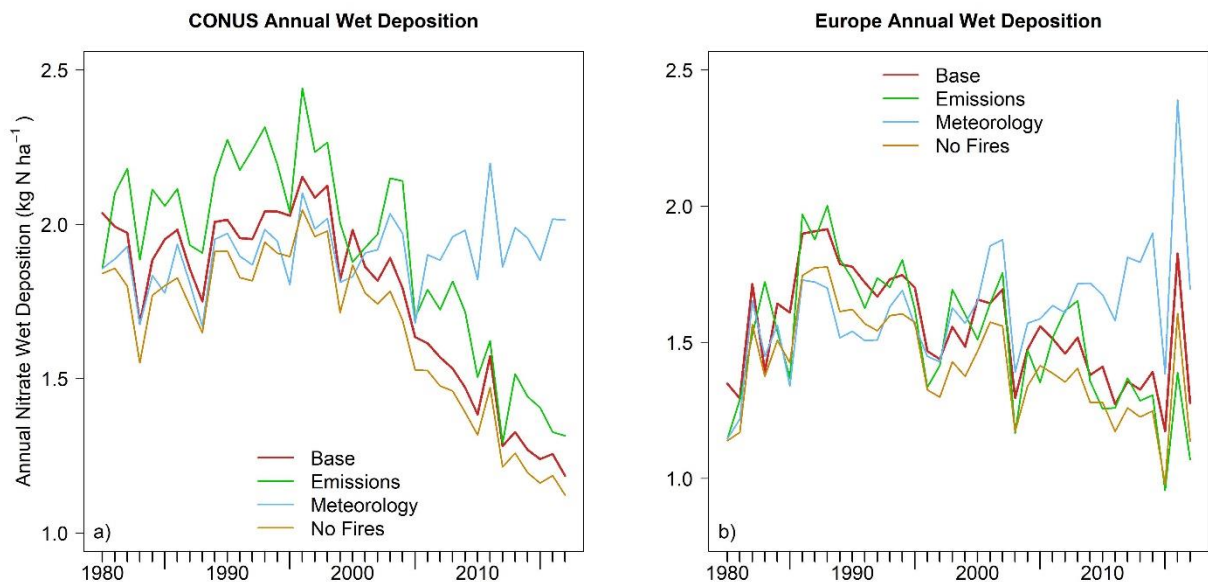
Figure 4. Results of annual NWD (kg N/ha) from each sensitivity simulation over (a) the CONUS and (b) Europe. The base GC simulation is shown in red, the simulation with changing emissions but constant meteorology (Emissions) is shown in green, the simulation with changing meteorology but constant anthropogenic emissions (Meteorology) is shown in blue, and the no biomass burning simulation (No Fires) is shown in gold. See Sect. 2.2 for a detailed description of these sensitivity runs.

Figure 5 shows anthropogenic NO_x emissions derived directly from the CEDS inventory (blue solid line) and total NO_x emissions summed using GEOS-Chem (black solid line), which includes all sources of NO_x emissions (anthropogenic from CEDS, soil, lightning, and biomass burning). Relative trends in observed NWD are overlaid (dashed purple line). In both the CONUS and Europe prior to 2010, NWD trends and NO_x emissions trends show good agreement in the model (R>=0.8). We find that the European trends generally show more noise, as there are far fewer sites over Europe than over the CONUS (28 vs 156 sites). Over both Europe and the CONUS, we find that annual trends in CEDS anthropogenic NO_x emissions agree well with NWD measurements until 2010, reflecting the strong decrease in anthropogenic emissions. After 2010, NWD decreases slow down in both the CONUS and Europe and reflect trends in total NO_x emissions. Over the CONUS, total NO_x emissions trends decline to -2.0 ± 1.8%/yr and NWD-predicted trends level out to -1.2 ± 2.9%/yr. Similarly, over Europe, total NO_x emissions trends decline to -0.5 ± 1.6%/yr after 2010, and NWD-predicted trends decline to -1.4 ± 3.6%/yr. As explored previously, these trends are in contrast to anthropogenic emissions inventories that continue to show strong NO_x decreases after 2010. These results point to the decreased influence of anthropogenic NO_x in total NO_x emissions trends and lend further evidence of the ability of NWD to capture total NO_x trends.
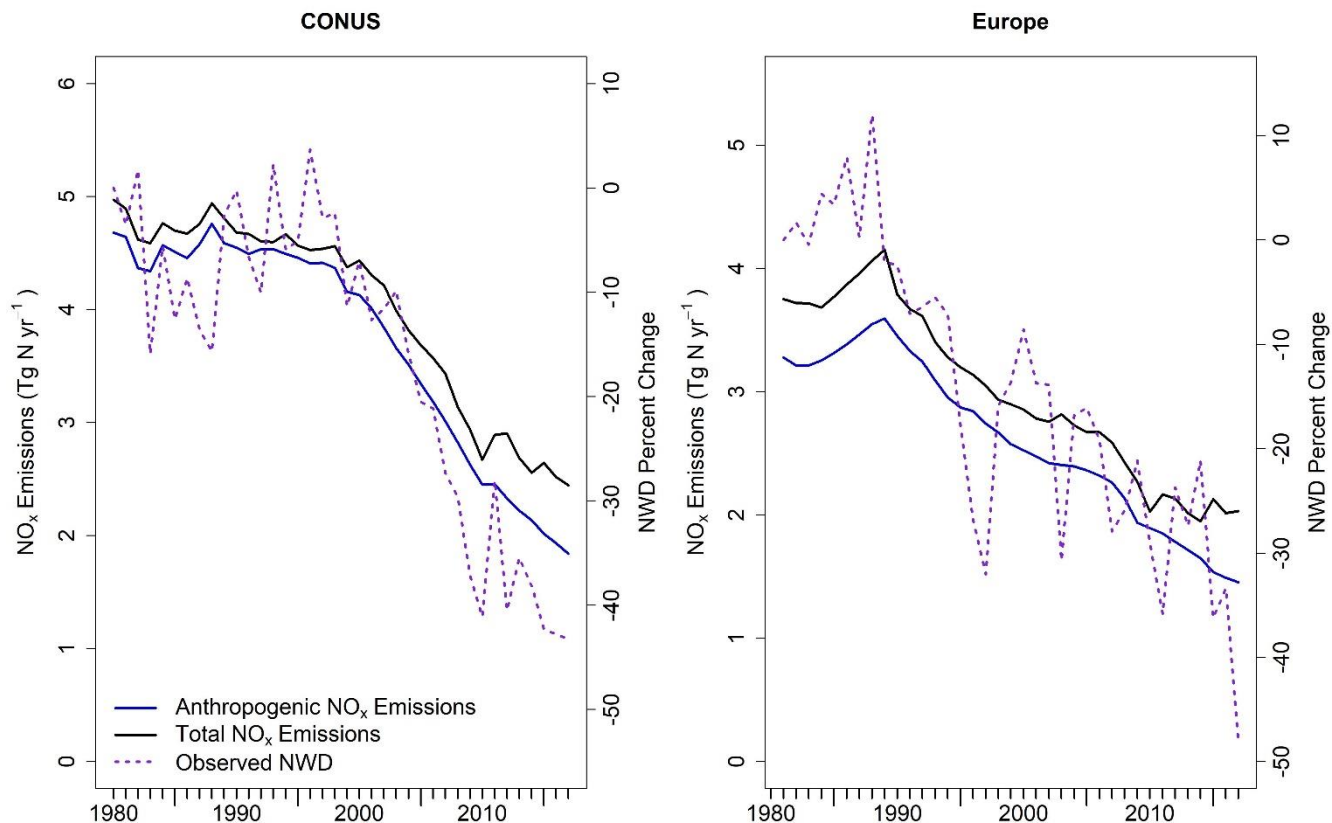
Figure 5. NOₓ trends in the CEDS inventory (reported as Tg N), total NOₓ emissions (Tg N) estimated by GEOS-Chem, and observed
415 **trends in annual NWD data over (a) the CONUS and (b) Europe. Anthropogenic emissions from the CEDS inventory are shown in solid blue, total NOₓ emissions are shown in black, and trends from NWD are overlaid with the dashed purple line.**

Through a series of sensitivity tests, we further illustrate this post-2010 flattening of the modelled total NOₓ emissions and observed NWD trends in response to the weakened sensitivity to anthropogenic emissions. We investigate the impact of a

420 small perturbation (-5%) in anthropogenic NOₓ emissions at various time points throughout the series (1985, 1995, 2000, 2005, 2013, and 2017) to investigate NWD sensitivity to a decrease in anthropogenic emissions (Table 2). We find that the sensitivity to anthropogenic NOₓ emissions is greatest in the 1980s and 1990s and decreases to its lowest sensitivity in 2017 over both the CONUS and Europe. This is in contrast to similar sensitivity simulations that reduced soil NOₓ emissions by 5%. In these simulations, NWD trends become slightly more sensitive to changes in background soil NOₓ emissions later in the timeframe,

425 especially over the CONUS. Our work underscores the value of measurements of NWD extending into the future for constraining total NOₓ trends.

Table 2. Sensitivity of modeled NWD to a 5% decrease in anthropogenic and soil NOₓ emissions at various time slices.

16

Year	NWD Reduction with 5% Anthro NO$_x$ Reduction (CONUS)	NWD Reduction with 5% Anthro NO$_x$ Reduction (Europe)	NWD Reduction with 5% Soil NO$_x$ Reduction (CONUS)	NWD Reduction with 5% Soil NO$_x$ Reduction (Europe)
1985	4.0%	4.9%	0.5%	0.2%
1995	4.2%	4.6%	0.5%	0.3%
2000	3.8%	4.5%	0.6%	0.3%
2005	4.0%	4.4%	0.5%	0.3%
2013	3.5%	4.2%	0.7%	0.3%
2017	3.3%	3.5%	0.7%	0.3%

430

3.3 Evidence of summertime NO$_x$ overestimates over the CONUS

In addition to its usefulness in assessing the total NO$_x$ trend, NWD can also provide insights into the accuracy of total NO$_x$ magnitudes in models. While annual NWD values agree when taken over the entire CONUS domain, regional NWD measurements suggest that NO$_x$ emissions are overestimated in certain regions and seasons. The eastern US has been the
435 subject of many studies related to the amount of NO$_x$ emissions, in which various versions of the NEI have been assessed using a variety of measurements. Multiple analyses have pointed to NO$_x$ overestimates in the NEI over the eastern US during summertime (Castellanos et al., 2011; Anderson et al., 2014; Goldberg et al., 2016; Souri et al., 2016; Travis et al., 2016), finding overestimates of 27% - 70% depending on location and time. We investigated potential similar biases in the CEDS inventory by comparing seasonal and regional measured and modeled NWD magnitudes.

440

Similar to previous analyses of NEI inventories, we find evidence of an overestimate of summertime (July-August-September or JAS) CEDS-estimated NO$_x$ across the entire CONUS from 1980-2017 (12% on average), but most prominently in the eastern US after 2000 (Fig. 6a). Overestimates in the eastern US average ~20% and range up to 77% after 2000. This implies that NO$_x$ emissions may be overestimated over the eastern US during JAS in the CEDS inventory and is consistent with
445 previous analyses of inventories with similar emissions. The CEDS inventory estimates that NO$_x$ emissions over the eastern US during JAS are 0.7 Tg N on average (0.9 Tg N in 1980 decreasing to 0.3 Tg N in 2017). These overestimates are likely present in other emissions inventories, such as the NEI 2017 and MACCity, as their emission trends and sizes over CONUS are similar across inventories (Fig. S4).
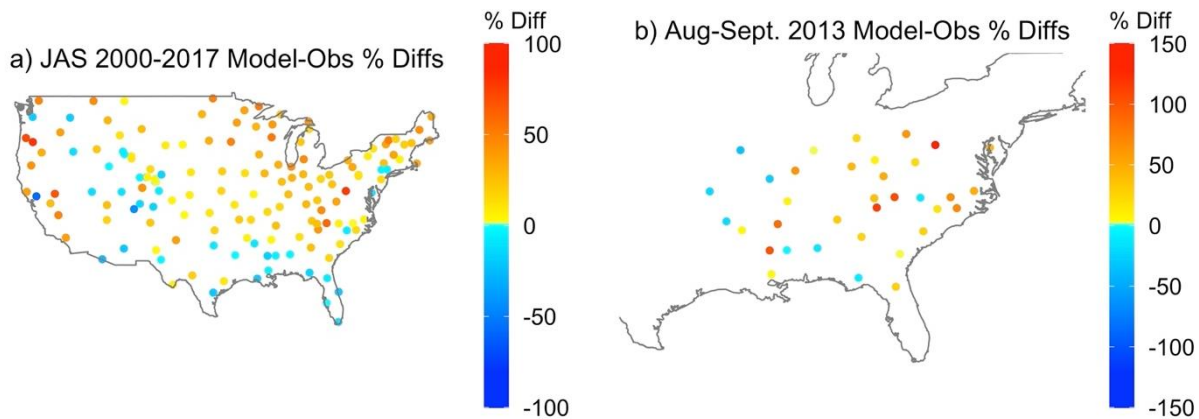
450

Figure 6. Modeled overestimates of (a) 2000-2010 summertime (JAS) NWD in the eastern US and (b) 2013 August-September NWD in the southeastern US, compared to the NADP observations. These overestimates likely signal that NO_x emissions over this region are overestimated by the CEDS inventory. Note that the scales are different between panels.

455 Further agreement for NO_x overestimates can be found by evaluating specific regions and timeframes where NO_x overestimates have been previously identified. For example, over the southeastern US during August-September 2013, Travis et al. (2016) showed that the NEI 2011 overestimated NO_x emissions by 71% compared to aircraft measurements. We examine the same area and time using modeled and measured NWD to investigate if the CEDS inventory is similarly overestimated in this region (Fig. 6b). We find that modeled NWD values using our GC simulation are ~30% higher than measured, implying that NO_x

460 emissions may be overestimated by 30% in the southeast US, qualitatively agreeing with Travis et al. (2016). CEDS NO_x emissions are slightly lower than the NEI 2011 by 15% over the southeastern US (CEDS estimate is 0.1 Tg N), which partially explains the difference in overestimates. The remaining discrepancy in overestimates may be accounted for through differences in model resolution. Travis et al. (2016) used 0.25°x0.25° horizontal resolution, while our model has 2°x2.5° resolution. Travis et al. (2016) attributed much of this overestimate to uncertainties in mobile and industrial sectors as they accounted for the

465 majority of the NO_x emissions in the model.

Overestimates of NO_x in emissions inventories extend beyond the eastern US. In the western US (longitudes west of 100° W) during summer (JAS), we find that modeled NWD fluxes are overestimated by 15% on average from 1980-2017, and these overestimates are consistent throughout the timeframe. This finding suggests that NO_x is slightly overestimated in the western

470 US during summer in CEDS, which estimates average emissions of 0.2 Tg N (range of 0.3 Tg N in 1980 to 0.1 Tg N in 2017). This is consistent with a previous analysis that found that the NEI 2005 overestimated NO_x in the Los Angeles area by 27-32% during May-June 2010 (Brioude et al., 2013).

18

During winter, we find much better agreement between regional modeled and measured NWD. NWD is slightly underestimated during winter in the eastern US (~7%). This good agreement in the eastern US is consistent with a previous study during winter in the Washington, D.C., and Baltimore area (WINTER) that showed the NEI 2011 and 2014 inventories were within measurement uncertainty from aircraft (Salmon et al., 2018; Jaeglé et al., 2018). In the western US, a worse agreement is generally seen, with overestimates averaging 11% during winter throughout the timeframe, but the standard deviation of the modeled and observed values overlap at each site.

The disagreement in NWD magnitudes during summer may also partially stem from overestimates of soil NO_x emissions in the model. Soil NO_x emissions are seasonal, with strong summertime emissions and small wintertime emissions. Soil NO_x contributes an average of 16% (ranging up to 26%) of total NO_x during summer and only 2% during winter. This seasonal pattern observed over the CONUS is consistent with a seasonal overestimate of NO_x, with summertime overestimates and good wintertime agreement. However, for most of the timeframe, the contribution of soil NO_x emissions cannot fully explain the observed overestimates that range up to 77%. Along with assessing anthropogenic NO_x emissions, future work should focus on refining soil emissions in models, especially as these background emissions become more important in determining total NO_x trends in countries with strongly decreasing anthropogenic NO_x. Similarly, potential overestimates of biomass burning cannot fully resolve the model-measurement discrepancy. Over the CONUS, excluding all biomass burning emissions globally (No Fires simulation) still results in summertime overestimates of NWD that average 12%, with overestimates in the eastern US averaging 13% and ranging up to 65%.

The sensitivity of NWD to anthropogenic NO_x emissions decreases from 1980-2017, and thus the relationship between anthropogenic NO_x and NWD is not strictly 1:1, although NWD is most sensitive to changes in anthropogenic NO_x emissions. This change in sensitivity can be attributed to the increasingly large role of background NO_x emissions to total NO_x, and changes in NO_x lifetime. It is more likely that these changes are better explained by the increasing prevalence of background NO_x, as a previous investigation of NO_x lifetime changes since the 2000s found that changes in lifetime alone cannot fully explain NO_x trends (Laughner and Cohen, 2019). Changes in NO_x lifetime impact NO_x product composition and phase, and future analyses should investigate the role of a changing NO_x lifetime on products such as nitric acid, nitrate aerosol, and organic nitrates.

It should be noted that the model does not overestimate NWD over all regions or seasons in the US. Some regions, such as the eastern US during spring, exhibit model underestimates. On an annual average basis across the CONUS, NWD is slightly overestimated, but certain regions and seasons show more prominent underestimates that should be explored more fully in future analyses (Fig. S6).

3.4 Evidence of widespread NO$_x$ overestimates over Europe

A recent analysis assessing NO$_x$ emissions over Europe via satellite measurements points out overestimates in Southern Europe during winter and across the entire European domain during summer (Szymankiewicz et al., 2021). The study suggested that EMEP anthropogenic NO$_x$ emissions needed to be reduced by 40% to match observations. Further, another study using OMI satellite NO$_2$ measurements found that ship emissions may be overestimated by 35-130% over Europe (Vinken et al., 2014). Here, we assess NWD overestimates seasonally and regionally to further assess potential NO$_x$ overestimates in the CEDS inventory. In this analysis, we use the meteorological definitions of the seasons: winter as December-January-February (DJF), spring as March-April-May (MAM), summer as June-July-August (JJA), and fall as September-October-November (SON).

Consistent with previous analyses, we find that overestimates of NO$_x$ occur throughout the European domain, but they are most prominent during summer (JJA) and fall (SON) (Fig. 7). Total anthropogenic NO$_x$ emissions over Europe are estimated by the CEDS inventory to be 2.6 Tg N on average (3.3 Tg N in 1980 declining to 1.5 Tg N in 2017). During summer and fall over the entire domain, we find that NWD is overestimated on average by 176% (50 to >500%, factor of 2.9 on average) and 169% (39 to >500%, factor of 2.7 on average), respectively, by the model. During winter and spring, this overestimate is smaller, but still ~100% (average factor of 2.4 and 1.9, respectively). These overestimates are strongest in central and southern Europe during winter and spring, but they exist throughout the domain during summer and fall. Anthropogenic NO$_x$ emissions make up the largest fraction of total NO$_x$ emissions from all sectors in the GC simulation, ranging from 74% to 88% of total emissions (Fig. S5). Therefore, it is most likely that overestimates of NWD stem from overestimates of anthropogenic NO$_x$ emissions rather than natural sources. In the CEDS inventory, the largest sector contribution to anthropogenic NO$_x$ is road emissions (39% of the total on average; Fig. S7), suggesting that overestimates may come from this sector.
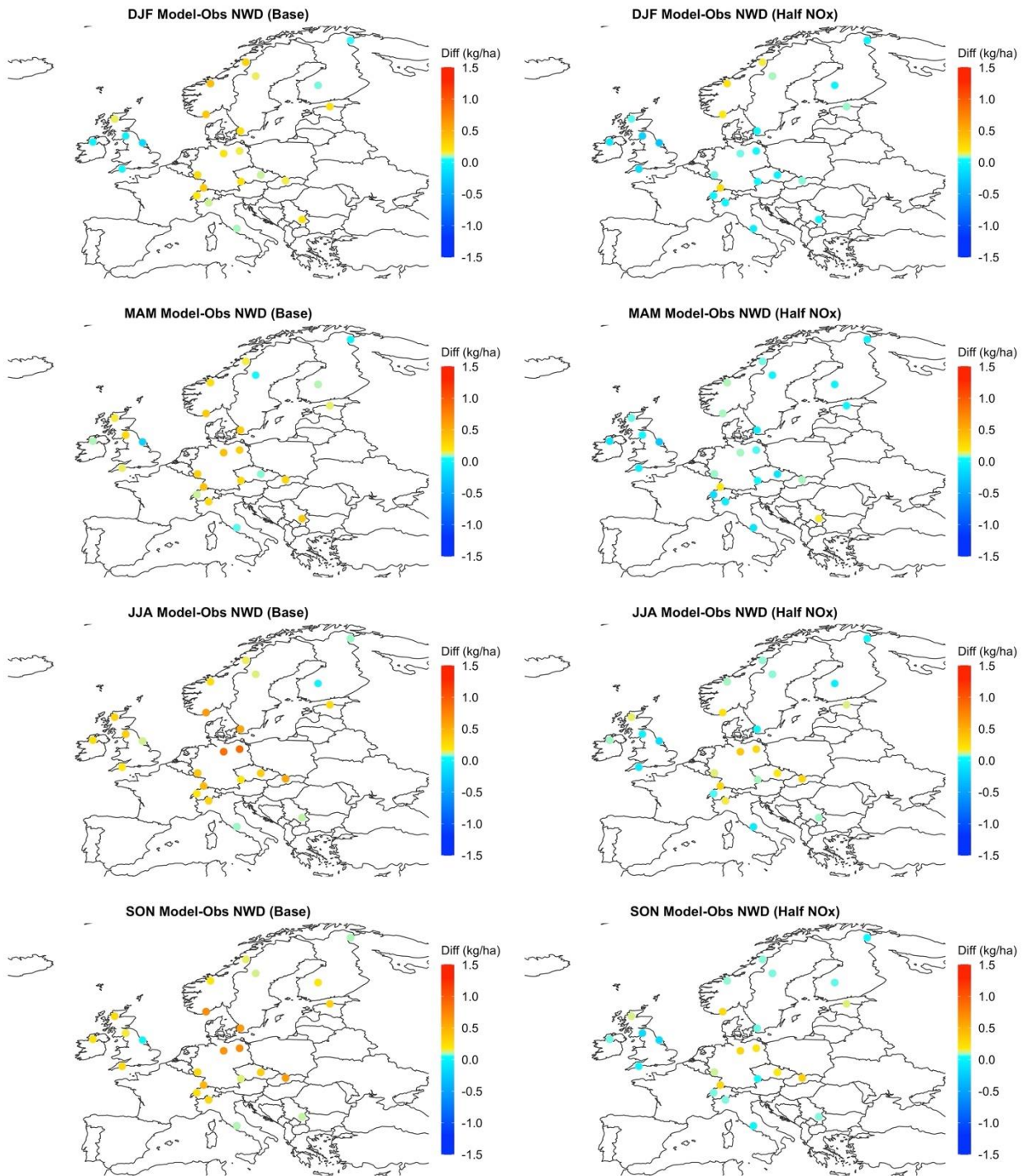
Figure 7. Model – observations differences in NWD (kg N ha⁻¹) in winter (DJF), spring (MAM), summer (JJA), and fall (SON). Warm colors indicate model overestimates. Differences between the base model results and observations are shown in the left panels, and the differences between the Half-NOx simulation and observations are shown in the right panels.

21

To test the impact of NO$_x$ emissions on model NWD, we perform a sensitivity test that cuts anthropogenic NO$_x$ emissions in the CEDS inventory in half (reducing the 1980-2017 average of 2.6 to 1.3 Tg N) over Europe using GC at the 4°x5° resolution (Fig. 7), as NO$_x$ and NWD correlate highly in all seasons (R>0.6). Halving NO$_x$ emissions also halves NWD fluxes over Europe, bringing the modeled NWD within 15% of observations on an annual basis (Fig. S8). However, we find that summertime and autumnal NO$_x$ is still overestimated by ~36% in the sensitivity simulation, suggesting that further reductions of NO$_x$ may be appropriate in certain areas during summer and fall (Fig. 7), and these seasonal corrections should be a focus of future work. Winter and springtime biases are practically eliminated, with average model-measurement differences of <10%. Anthropogenic NO$_x$ over Europe is overestimated by the CEDS inventory, especially in central and southern Europe during summer and fall. These overestimates likely extend to other inventories that show similar NO$_x$ emissions magnitudes, trends, and spatial distribution (e.g., MACCity, EMEP; Fig. S4).

As discussed previously for the CONUS, it is also possible that this disagreement in NWD magnitudes in Europe during summer stems partially from overestimates of soil NO$_x$ in the model. However, this difference is not large enough to fully explain these overestimates, as soil NO$_x$ emissions range from <2 to 23% of total NO$_x$ emissions over Europe. The elimination of global biomass burning emissions in the No-Fires simulation also does not resolve this discrepancy. On average, NWD overestimates in this simulation over Europe still average 115% year-round, with overestimates of 145% in summer and 140% in fall in our No Fires simulation.

4 Impacts of NO$_x$ emissions changes on tropospheric ozone concentrations

Adjusting NO$_x$ emissions impacts ozone concentrations, and NO$_x$ is currently one of the largest uncertainties regarding model reproduction of ozone concentrations and trends. Currently, summertime ozone is overestimated at the surface over Europe in GEOS-Chem (Christiansen et al., 2022). GEOS-Chem also overestimates surface ozone over the CONUS at locations in the TOAR database by 8% on average during summer and fall. Other studies have suggested that this may be due to NO$_x$ overestimates in regional anthropogenic inventories, issues in vertical mixing representation, excessive model biogenic VOC production, or missing sinks (Travis et al., 2016; Guo et al., 2018). Regional and seasonal overestimates in NO$_x$ emissions discussed in Sect. 3.3 may also contribute to these ozone overestimates. While we did not explore these sensitivities in this work, future efforts should focus on constraining potential NO$_x$ overestimates in the US that may contribute to model ozone discrepancies.

We find that reducing anthropogenic NO$_x$ emissions over Europe by half results in an average decrease in summertime ozone concentrations of 14% (7 ppb) during summer below 700 hPa (Fig. 8). At the surface, this reduction in anthropogenic NO$_x$ emissions improves model reproduction of ozone compared to observations (Fig. 8). The surface ozone overestimate over

Europe is reduced from 14% (6 ppb) to 2% (0.7 ppb) on average, bringing it within agreement of observations. Further, this adjustment improves the representation of downwind sites in Eurasia, reducing average summertime overestimates from 14% to 7%. It is important to note that this analysis was done on a regional scale. Ozone formation varies between urban and rural regions, where formation regimes can switch between NO_x- and VOC-limited over a short spatial scale. Future analyses should investigate the impact of NO_x constraints on model ozone at the urban scale.
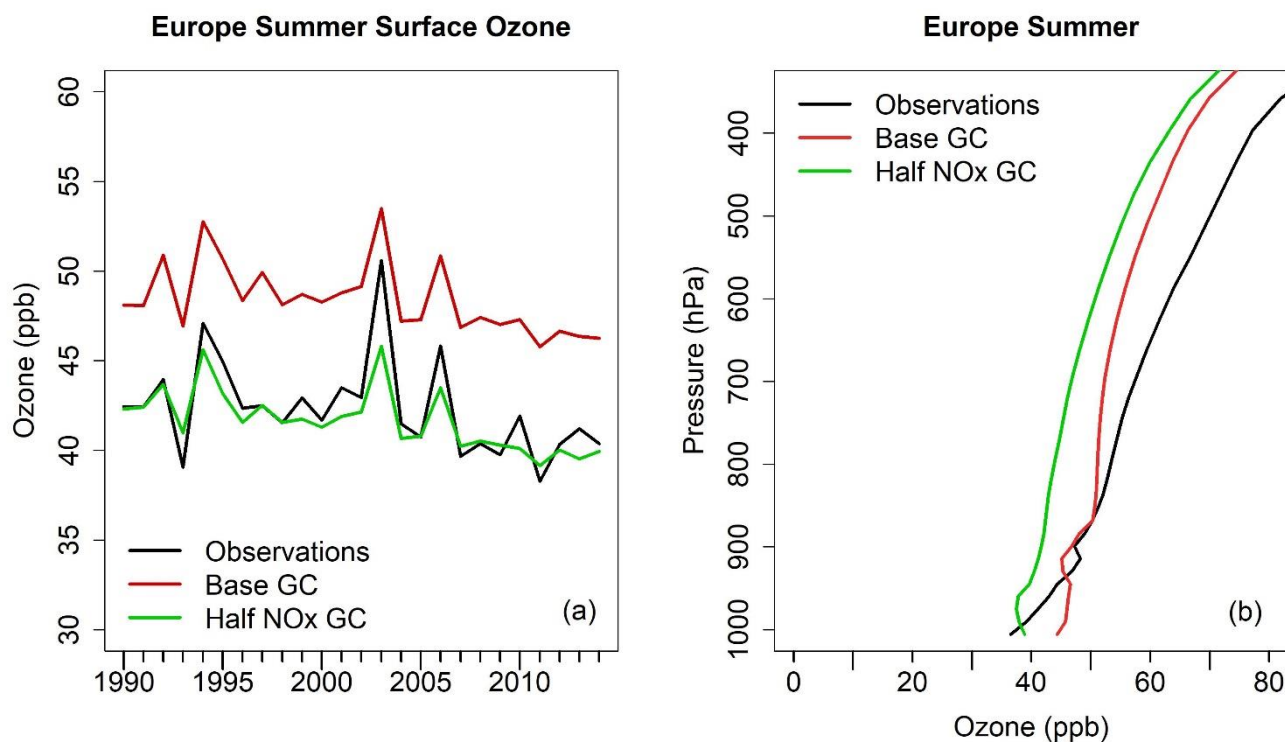
Figure 8. Comparisons between observed and modeled summertime ozone concentrations, averaged over Europe. Results from the Half-NO_x sensitivity simulation are also shown. (a) Observations of surface ozone compiled by the TOAR Database team (Schultz et al., 2017) are shown in black, GC surface ozone is shown in red, and surface ozone from the Half-NO_x simulation is shown in green. (b) Vertical profiles of ozone observed by WOUDC and HEGIFTOM are shown in black, GC ozone is shown in red, and ozone from our Half-NO_x simulation is shown in green. The vertical profiles are an average of summertime concentrations from 1990-2017. GC was sampled at the same launch time and location as all ozonesonde launches compiled here.

Above the surface, however, these ozone reductions do not improve model representation of ozone in Europe, instead further exacerbating existing underestimates. Figure 8 shows tropospheric ozone extending through the free troposphere over Europe during summer before and after NO_x emissions reductions compared to ozonesonde measurements compiled by WOUDC and HEGIFTOM. Recent versions of GEOS-Chem record systemically low model ozone burdens, especially in the northern mid-latitude free troposphere, most notably in winter and spring (Mao et al., 2021; Murray et al., 2021; Christiansen et al., 2022).

GC underestimates ozone by ~10 ppb in the mid-latitude free troposphere (Christiansen et al., 2022). Reasons for these underestimates have been explored in depth recently. Briefly, model updates including more active halogen chemistry (Wang et al., 2021), increased NO_y reactive uptake by clouds (Holmes et al., 2019), and underestimates of lightning-produced oxidants (Mao et al., 2021) all contribute to these systemic ozone underestimates, even as they improve the model's representation of different chemical processes in the troposphere. Such underestimates are not present in other chemical transport models, including MERRA2-GMI from NASA (http://acd-ext.gsfc.nasa.gov/Projects/GEOSCCM/MERRA2GMI; last access: 21 Dec 2023) and the previous version of GEOS-Chem explored in this work (v10-01), that do not include these updates (Christiansen et al., 2022). Future work is needed to update model chemistry and emissions to bring free tropospheric ozone in line with observations. A recent study suggested that inclusion of particulate nitrate could also help reduce this bias by up to 5 ppb in the northern extratropics (Shah et al., 2022).

5 Conclusions

In this work, we provided a new, independent constraint on NO_x emissions and trends over the United States and Europe using NWD flux measurements. We found that anthropogenic NO_x trends in the CEDS emissions inventory are reproduced well by NWD until 2010, and that total (i.e., anthropogenic + lightning + soils + biomass burning) NO_x emission trends are well reproduced by NWD after 2010. NWD trends are also capable of reproducing the large drop in NO_x emissions during COVID-19 lockdowns, and NWD magnitudes are consistent with analyses from satellite and surface NO_2 measurements, demonstrating the value of NWD in constraining NO_x emission changes. NWD observations show a leveling off of decreasing trends after 2010 consistent with satellite measurements, suggesting the increasing importance of background NO_x emissions in determining total NO_x trends. We provided further evidence that NWD fluxes are becoming less sensitive to changes in anthropogenic emissions via sensitivity simulations in GEOS-Chem. We also used simulations of NWD via GEOS-Chem to provide evidence of potential overestimates in anthropogenic NO_x emissions in standard inventories. While annual trends in the model over the CONUS agree well with observed NWD, we found that NWD magnitudes were overestimated during summer by an average of 20% over the eastern US after 2000. We also found evidence of widespread NO_x overestimates in CEDS (factor of >2) over Europe that persist in all seasons but are strongest during summer and fall. Some of the overestimates in these regions may be due to uncertainties in soil NO_x estimates, although these emissions are too small to fully explain the discrepancy. Reducing anthropogenic NO_x emissions by 50% in the GEOS-Chem+CEDS simulation brings winter and springtime fluxes within 10% of measurements, but summer and fall NWD are still overestimated by ~36%. These NO_x emission reductions also improve model simulations of surface ozone, decreasing the summertime overestimate over Europe from 14% to 2%, but do not improve model free tropospheric ozone biases. Our work shows that NWD fluxes can be a useful constraint on total (anthropogenic + background) NO_x emissions and trends (rapid decrease from 1990-2010, and flattening after 2010), especially as anthropogenic NO_x emissions continue to decrease in countries with strict emissions regulations and

24

accurate representation of background sources of NO_x becomes necessary to fully understand trends. Due to the model resolutions used here, these findings are most relevant at the regional scale, and future analyses should focus on smaller spatial and temporal (e.g., seasonal) scales to further refine NWD as an independent NO_x constraint.

Data and code availability

Data and R code used in this publication are available at https://doi.org/10.5281/zenodo.8141028. The GEOS-Chem model is publicly available at https://doi.org/10.5281/zenodo.3974569. Publicly available nitrate wet deposition can be found at https://nadp.slh.wisc.edu/networks/national-trends-network/ for NADP and https://ebas.nilu.no/data-access/ for EMEP. High resolution precipitation datasets are available at https://prism.oregonstate.edu/ and https://surfobs.climate.copernicus.eu/surfobs.php. Publicly available surface ozone is available from the TOAR network at https://doi.pangaea.de/10.1594/PANGAEA.876108, and publicly available ozonesonde information is available at https://doi.org/10.14287/10000001 with updates from HEGIFTOM at https://hegiftom.meteo.be/datasets/ozonesondes.

Author contributions

LH and LJM designed the research. AC performed GEOS-Chem v12.9.3 model simulations, data analysis, and wrote the paper. LH performed the GEOS-Chem v10-01 model simulation.

Competing interests

The authors declare that they have no conflict of interest.

References

Ancellet, G., Godin-Beekmann, S., Smit, H. G. J., Stauffer, R. M., Van Malderen, R., Bodichon, R., and Pazmiño, A.: Homogenization of the Observatoire de Haute Provence electrochemical concentration cell (ECC) ozonesonde data record: comparison with lidar and satellite observations, Atmos. Meas. Tech., 15, https://doi.org/10.5194/amt-15-3105-2022, 2022.

Anderson, D. C., Loughner, C. P., Diskin, G., Weinheimer, A., Canty, T. P., Salawitch, R. J., Worden, H. M., Fried, A., Mikoviny, T., Wisthaler, A., and Dickerson, R. R.: Measured and modeled CO and NO y in DISCOVER-AQ: An evaluation of emissions and chemistry over the eastern US, Atmospheric Environment, 96, 78–87, https://doi.org/10.1016/j.atmosenv.2014.07.004, 2014.

Baldasano, J. M.: COVID-19 lockdown effects on air quality by NO2 in the cities of Barcelona and Madrid (Spain), Science of The Total Environment, 741, 140353, https://doi.org/10.1016/j.scitotenv.2020.140353, 2020.

Bar, S., Parida, B. R., Mandal, S. P., Pandey, A. C., Kumar, N., and Mishra, B.: Impacts of partial to complete COVID-19 lockdown on NO2 and PM2.5 levels in major urban cities of Europe and USA, Cities, 117, 103308, https://doi.org/10.1016/j.cities.2021.103308, 2021.

Barkley, M. P., González Abad, G., Kurosu, T. P., Spurr, R., Torbatian, S., and Lerot, C.: OMI air-quality monitoring over the Middle East, Atmos. Chem. Phys., 17, 4687–4709, https://doi.org/10.5194/acp-17-4687-2017, 2017.

Bates, K. H. and Jacob, D. J.: A new model mechanism for atmospheric oxidation of isoprene: global effects on oxidants, nitrogen oxides, organic products, and secondary organic aerosol, Atmos. Chem. Phys., 19, 9613–9640, https://doi.org/10.5194/acp-19-9613-2019, 2019.

Bauwens, M., Compernolle, S., Stavrakou, T., Müller, J. -F., Gent, J., Eskes, H., Levelt, P. F., A, R., Veefkind, J. P., Vlietinck, J., Yu, H., and Zehner, C.: Impact of Coronavirus Outbreak on NO2 Pollution Assessed Using TROPOMI and OMI Observations, Geophys. Res. Lett., 47, https://doi.org/10.1029/2020GL087978, 2020.

Bell, M. L., Peng, R. D., and Dominici, F.: The Exposure–Response Curve for Ozone and Risk of Mortality and the Adequacy of Current Ozone Regulations, Environmental Health Perspectives, 114, 532–536, https://doi.org/10.1289/ehp.8816, 2006.

Bey, I., Jacob, D. J., Yantosca, R. M., Logan, J. A., Field, B. D., Fiore, A. M., Li, Q., Liu, H. Y., Mickley, L. J., and Schultz, M. G.: Global modeling of tropospheric chemistry with assimilated meteorology: Model description and evaluation, J. Geophys. Res., 106, 23073–23095, https://doi.org/10.1029/2001JD000807, 2001.

Brioude, J., Angevine, W. M., Ahmadov, R., Kim, S.-W., Evan, S., McKeen, S. A., Hsie, E.-Y., Frost, G. J., Neuman, J. A., Pollack, I. B., Peischl, J., Ryerson, T. B., Holloway, J., Brown, S. S., Nowak, J. B., Roberts, J. M., Wofsy, S. C., Santoni, G. W., Oda, T., and Trainer, M.: Top-down estimate of surface flux in the Los Angeles Basin using a mesoscale inverse modeling technique: assessing anthropogenic emissions of CO, NO_x and CO_2 and their impacts, Atmos. Chem. Phys., 13, 3661–3677, https://doi.org/10.5194/acp-13-3661-2013, 2013.

Burnett, R. T., Pope, C. A., III, Ezzati, M., Olives, C., Lim, S. S., Mehta, S., Shin, H. H., Singh, G., Hubbell, B., Brauer, M., Anderson, H. R., Smith, K. R., Balmes, J. R., Bruce, N. G., Kan, H., Laden, F., Prüss-Ustün, A., Turner, M. C., Gapstur, S. M., Diver, W. R., and Cohen, A.: An Integrated Risk Function for Estimating the Global Burden of Disease Attributable to Ambient Fine Particulate Matter Exposure, Environmental Health Perspectives, https://doi.org/10.1289/ehp.1307049, 2014.

Butler, T. J., Likens, G. E., Vermeylen, F. M., and Stunder, B. J. B.: The relation between NOx emissions and precipitation NO3− in the eastern USA, Atmospheric Environment, 37, 2093–2104, https://doi.org/10.1016/S1352-2310(03)00103-1, 2003.

Canty, T. P., Hembeck, L., Vinciguerra, T. P., Anderson, D. C., Goldberg, D. L., Carpenter, S. F., Allen, D. J., Loughner, C. P., Salawitch, R. J., and Dickerson, R. R.: Ozone and NOx chemistry in the eastern US: evaluation of CMAQ/CB05 with satellite (OMI) data, Atmos. Chem. Phys., 15, 10965–10982, https://doi.org/10.5194/acp-15-10965-2015, 2015.

Castellanos, P., Marufu, L. T., Doddridge, B. G., Taubman, B. F., Schwab, J. J., Hains, J. C., Ehrman, S. H., and Dickerson, R. R.: Ozone, oxides of nitrogen, and carbon monoxide during pollution events over the eastern United States: An evaluation of emissions and vertical mixing, J. Geophys. Res., 116, D16307, https://doi.org/10.1029/2010JD014540, 2011.

Christiansen, A., Mickley, L. J., Liu, J., Oman, L. D., and Hu, L.: Multidecadal increases in global tropospheric ozone derived from ozonesonde and surface site observations: can models reproduce ozone trends?, Atmos. Chem. Phys., 22, 14751–14782, https://doi.org/10.5194/acp-22-14751-2022, 2022.

Dallmann, T. R. and Harley, R. A.: Evaluation of mobile source emission trends in the United States, J. Geophys. Res., 115, D14305, https://doi.org/10.1029/2010JD013862, 2010.

Daly, C., Halbleib, M., Smith, J. I., Gibson, W. P., Doggett, M. K., Taylor, G. H., Curtis, J., and Pasteris, P. P.: Physiographically sensitive mapping of climatological temperature and precipitation across the conterminous United States, Int. J. Climatol., 28, 2031–2064, https://doi.org/10.1002/joc.1688, 2008.

Du, E., de Vries, W., Galloway, J. N., Hu, X., and Fang, J.: Changes in wet nitrogen deposition in the United States between 1985 and 2012, Environ. Res. Lett., 9, 095004, https://doi.org/10.1088/1748-9326/9/9/095004, 2014.

Duncan, B. N.: Interannual and seasonal variability of biomass burning emissions constrained by satellite observations, J. Geophys. Res., 108, 4100, https://doi.org/10.1029/2002JD002378, 2003.

715 Duncan, B. N., Lamsal, L. N., Thompson, A. M., Yoshida, Y., Lu, Z., Streets, D. G., Hurwitz, M. M., and Pickering, K. E.: A space-based, high-resolution view of notable changes in urban NO_x pollution around the world (2005-2014): NOTABLE CHANGES IN URBAN NO_X POLLUTION, J. Geophys. Res. Atmos., 121, 976–996, https://doi.org/10.1002/2015JD024121, 2016.

Dutta, I. and Heald, C. L.: Exploring Deposition Observations of Oxidized Sulfur and Nitrogen as a 720 Constraint on Emissions in the United States, JGR Atmospheres, 128, e2023JD039610, https://doi.org/10.1029/2023JD039610, 2023.

Elguindi, N., Granier, C., Stavrakou, T., Darras, S., Bauwens, M., Cao, H., Chen, C., Denier van der Gon, H. A. C., Dubovik, O., Fu, T. M., Henze, D. K., Jiang, Z., Keita, S., Kuenen, J. J. P., Kurokawa, J., Liousse, C., Miyazaki, K., Müller, J. -F., Qu, Z., Solmon, F., and Zheng, B.: Intercomparison of 725 Magnitudes and Trends in Anthropogenic Surface Emissions From Bottom-Up Inventories, Top-Down Estimates, and Emission Scenarios, Earth's Future, 8, https://doi.org/10.1029/2020EF001520, 2020.

Finkelstein, P. L., Ellestad, T. G., Clarke, J. F., Meyers, T. P., Schwede, D. B., Hebert, E. O., and Neal, J. A.: Ozone and sulfur dioxide dry deposition to forests: Observations and model evaluation, J. Geophys. Res., 105, 15365–15377, https://doi.org/10.1029/2000JD900185, 2000.

730 Frost, G. J., McKeen, S. A., Trainer, M., Ryerson, T. B., Neuman, J. A., Roberts, J. M., Swanson, A., Holloway, J. S., Sueper, D. T., Fortin, T., Parrish, D. D., Fehsenfeld, F. C., Flocke, F., Peckham, S. E., Grell, G. A., Kowal, D., Cartwright, J., Auerbach, N., and Habermann, T.: Effects of changing power plant NO_x emissions on ozone in the eastern United States: Proof of concept, J. Geophys. Res., 111, D12306, https://doi.org/10.1029/2005JD006354, 2006.

735 Galloway, J. N., Aber, J. D., Erisman, J. W., Seitzinger, S. P., Howarth, R. W., Cowling, E. B., and Cosby, B. J.: The Nitrogen Cascade, BioScience, 53, 341, https://doi.org/10.1641/0006-3568(2003)053[0341:TNC]2.0.CO;2, 2003.

Gauderman, W. J., Avol, E., Lurmann, F., Kuenzli, N., Gilliland, F., Peters, J., and McConnell, R.: Childhood Asthma and Exposure to Traffic and Nitrogen Dioxide, Epidemiology, 16, 737–743, 2005.

740 Gelaro, R., McCarty, W., Suárez, M. J., Todling, R., Molod, A., Takacs, L., Randles, C. A., Darmenov, A., Bosilovich, M. G., Reichle, R., Wargan, K., Coy, L., Cullather, R., Draper, C., Akella, S., Buchard, V., Conaty, A., da Silva, A. M., Gu, W., Kim, G.-K., Koster, R., Lucchesi, R., Merkova, D., Nielsen, J. E., Partyka, G., Pawson, S., Putman, W., Rienecker, M., Schubert, S. D., Sienkiewicz, M., and Zhao, B.: The Modern-Era Retrospective Analysis for Research and Applications, Version 2 (MERRA-2), Journal 745 of Climate, 30, 5419–5454, https://doi.org/10.1175/JCLI-D-16-0758.1, 2017.

Giglio, L., Randerson, J. T., and van der Werf, G. R.: Analysis of daily, monthly, and annual burned area using the fourth-generation global fire emissions database (GFED4): ANALYSIS OF BURNED AREA, J. Geophys. Res. Biogeosci., 118, 317–328, https://doi.org/10.1002/jgrg.20042, 2013.

Goldberg, D. L., Vinciguerra, T. P., Anderson, D. C., Hembeck, L., Canty, T. P., Ehrman, S. H., Martins, D. K., Stauffer, R. M., Thompson, A. M., Salawitch, R. J., and Dickerson, R. R.: CAMx ozone source attribution in the eastern United States using guidance from observations during DISCOVER-AQ Maryland: CAMX OZONE SOURCE ATTRIBUTION, Geophys. Res. Lett., 43, 2249–2258, https://doi.org/10.1002/2015GL067332, 2016.

Goldberg, D. L., Lu, Z., Streets, D. G., de Foy, B., Griffin, D., McLinden, C. A., Lamsal, L. N., Krotkov, N. A., and Eskes, H.: Enhanced Capabilities of TROPOMI NO_2: Estimating NO_x from North American Cities and Power Plants, Environ. Sci. Technol., 53, 12594–12601, https://doi.org/10.1021/acs.est.9b04488, 2019.

Goldberg, D. L., Anenberg, S. C., Lu, Z., Streets, D. G., Lamsal, L. N., E McDuffie, E., and Smith, S. J.: Urban NO_x emissions around the world declined faster than anticipated between 2005 and 2019, Environ. Res. Lett., 16, 115004, https://doi.org/10.1088/1748-9326/ac2c34, 2021.

Granier, C., Bessagnet, B., Bond, T., D'Angiola, A., Denier van der Gon, H., Frost, G. J., Heil, A., Kaiser, J. W., Kinne, S., Klimont, Z., Kloster, S., Lamarque, J.-F., Liousse, C., Masui, T., Meleux, F., Mieville, A., Ohara, T., Raut, J.-C., Riahi, K., Schultz, M. G., Smith, S. J., Thompson, A., van Aardenne, J., van der Werf, G. R., and van Vuuren, D. P.: Evolution of anthropogenic and biomass burning emissions of air pollutants at global and regional scales during the 1980–2010 period, Climatic Change, 109, 163–190, https://doi.org/10.1007/s10584-011-0154-1, 2011.

Guenther, A. B., Jiang, X., Heald, C. L., Sakulyanontvittaya, T., Duhl, T., Emmons, L. K., and Wang, X.: The Model of Emissions of Gases and Aerosols from Nature version 2.1 (MEGAN2.1): an extended and updated framework for modeling biogenic emissions, Geoscientific Model Development, 5, 1471–1492, https://doi.org/10.5194/gmd-5-1471-2012, 2012.

Guo, J. J., Fiore, A. M., Murray, L. T., Jaffe, D. A., Schnell, J. L., Moore, C. T., and Milly, G. P.: Average versus high surface ozone levels over the continental USA: model bias, background influences, and interannual variability, Atmos. Chem. Phys., 18, 12123–12140, https://doi.org/10.5194/acp-18-12123-2018, 2018.

Harkins, C., McDonald, B. C., Henze, D. K., and Wiedinmyer, C.: A fuel-based method for updating mobile source emissions during the COVID-19 pandemic, Environ. Res. Lett., 16, 065018, https://doi.org/10.1088/1748-9326/ac0660, 2021.

Haylock, M. R., Hofstra, N., Klein Tank, A. M. G., Klok, E. J., Jones, P. D., and New, M.: A European daily high-resolution gridded data set of surface temperature and precipitation for 1950–2006, J. Geophys. Res., 113, D20119, https://doi.org/10.1029/2008JD010201, 2008.

He, T., Jones, D. B. A., Miyazaki, K., Huang, B., Liu, Y., Jiang, Z., White, E. C., Worden, H. M., and Worden, J. R.: Deep Learning to Evaluate US NO $_x$ Emissions Using Surface Ozone Predictions, JGR Atmospheres, 127, https://doi.org/10.1029/2021JD035597, 2022.

Hoesly, R. M., Smith, S. J., Feng, L., Klimont, Z., Janssens-Maenhout, G., Pitkanen, T., Seibert, J. J., Vu, L., Andres, R. J., Bolt, R. M., Bond, T. C., Dawidowski, L., Kholod, N., Kurokawa, J., Li, M., Liu, L., Lu, Z., Moura, M. C. P., O'Rourke, P. R., and Zhang, Q.: Historical (1750–2014) anthropogenic emissions of reactive gases and aerosols from the Community Emissions Data System (CEDS), Geosci. Model Dev., 11, 369–408, https://doi.org/10.5194/gmd-11-369-2018, 2018.

Holmes, C. D., Bertram, T. H., Confer, K. L., Graham, K. A., Ronan, A. C., Wirks, C. K., and Shah, V.: The Role of Clouds in the Tropospheric NO $_x$ Cycle: A New Modeling Approach for Cloud Chemistry and Its Global Implications, Geophys. Res. Lett., 46, 4980–4990, https://doi.org/10.1029/2019GL081990, 2019.

Hu, L., Millet, D. B., Baasandorj, M., Griffis, T. J., Turner, P., Helmig, D., Curtis, A. J., and Hueber, J.: Isoprene emissions and impacts over an ecological transition region in the U.S. Upper Midwest inferred from tall tower measurements: Isoprene emissions in US Upper Midwest, J. Geophys. Res. Atmos., 120, 3553–3571, https://doi.org/10.1002/2014JD022732, 2015.

Hu, L., Jacob, D. J., Liu, X., Zhang, Y., Zhang, L., Kim, P. S., Sulprizio, M. P., and Yantosca, R. M.: Global budget of tropospheric ozone: Evaluating recent model advances with satellite (OMI), aircraft (IAGOS), and ozonesonde observations, Atmospheric Environment, 167, 323–334, https://doi.org/10.1016/j.atmosenv.2017.08.036, 2017.

Hudman, R. C., Moore, N. E., Mebust, A. K., Martin, R. V., Russell, A. R., Valin, L. C., and Cohen, R. C.: Steps towards a mechanistic model of global soil nitric oxide emissions: implementation and space based-constraints, Atmos. Chem. Phys., 12, 7779–7795, https://doi.org/10.5194/acp-12-7779-2012, 2012.

Jaeglé, L., Shah, V., Thornton, J. A., Lopez-Hilfiker, F. D., Lee, B. H., McDuffie, E. E., Fibiger, D., Brown, S. S., Veres, P., Sparks, T. L., Ebben, C. J., Wooldridge, P. J., Kenagy, H. S., Cohen, R. C., Weinheimer, A. J., Campos, T. L., Montzka, D. D., Digangi, J. P., Wolfe, G. M., Hanisco, T., Schroder, J. C., Campuzano-Jost, P., Day, D. A., Jimenez, J. L., Sullivan, A. P., Guo, H., and Weber, R. J.: Nitrogen Oxides Emissions, Chemistry, Deposition, and Export Over the Northeast United States During the WINTER Aircraft Campaign, J. Geophys. Res. Atmos., 123, https://doi.org/10.1029/2018JD029133, 2018.

Jiang, Z., Jones, D. B. A., Worden, H. M., Deeter, M. N., Henze, D. K., Worden, J., Bowman, K. W., Brenninkmeijer, C. A. M., and Schuck, T. J.: Impact of model errors in convective transport on CO source estimates inferred from MOPITT CO retrievals: EFFECT OF CONVECTION ON INVERSION, J. Geophys. Res. Atmos., 118, 2073–2083, https://doi.org/10.1002/jgrd.50216, 2013.

Jiang, Z., McDonald, B. C., Worden, H., Worden, J. R., Miyazaki, K., Qu, Z., Henze, D. K., Jones, D. B. A., Arellano, A. F., Fischer, E. V., Zhu, L., and Boersma, K. F.: Unexpected slowdown of US pollutant emission reduction in the past decade, Proc Natl Acad Sci USA, 115, 5099–5104, https://doi.org/10.1073/pnas.1801191115, 2018.

820 Keller, C. A., Long, M. S., Yantosca, R. M., Da Silva, A. M., Pawson, S., and Jacob, D. J.: HEMCO v1.0: a versatile, ESMF-compliant component for calculating emissions in atmospheric models, Geosci. Model Dev., 7, 1409–1417, https://doi.org/10.5194/gmd-7-1409-2014, 2014.

Kenagy, H. S., Sparks, T. L., Ebben, C. J., Wooldrige, P. J., Lopez-Hilfiker, F. D., Lee, B. H., Thornton, J. A., McDuffie, E. E., Fibiger, D. L., Brown, S. S., Montzka, D. D., Weinheimer, A. J., Schroder, J. C., 825 Campuzano-Jost, P., Day, D. A., Jimenez, J. L., Dibb, J. E., Campos, T., Shah, V., Jaeglé, L., and Cohen, R. C.: NO$_x$ Lifetime and NO$_y$ Partitioning During WINTER, J. Geophys. Res. Atmos., 123, 9813–9827, https://doi.org/10.1029/2018JD028736, 2018.

Kerr, G. H., Goldberg, D. L., and Anenberg, S. C.: COVID-19 pandemic reveals persistent disparities in nitrogen dioxide pollution, Proc. Natl. Acad. Sci. U.S.A., 118, e2022409118, 830 https://doi.org/10.1073/pnas.2022409118, 2021.

Kota, S. H., Zhang, H., Chen, G., Schade, G. W., and Ying, Q.: Evaluation of on-road vehicle CO and NOx National Emission Inventories using an urban-scale source-oriented air quality model, Atmospheric Environment, 85, 99–108, https://doi.org/10.1016/j.atmosenv.2013.11.020, 2014.

Krotkov, N. A., McLinden, C. A., Li, C., Lamsal, L. N., Celarier, E. A., Marchenko, S. V., Swartz, W. 835 H., Bucsela, E. J., Joiner, J., Duncan, B. N., Boersma, K. F., Veefkind, J. P., Levelt, P. F., Fioletov, V. E., Dickerson, R. R., He, H., Lu, Z., and Streets, D. G.: Aura OMI observations of regional SO$_2$ and NO$_2$ pollution changes from 2005 to 2015, Atmos. Chem. Phys., 16, 4605–4629, https://doi.org/10.5194/acp-16-4605-2016, 2016.

Krotkov, N. A., Lamsal, L. N., Celarier, E. A., Swartz, W. H., Marchenko, S. V., Bucsela, E. J., Chan, K. 840 L., Wenig, M., and Zara, M.: The version 3 OMI NO$_2$ standard product, Atmos. Meas. Tech., 10, 3133–3149, https://doi.org/10.5194/amt-10-3133-2017, 2017.

Lamb, D. and Bowersox, V.: The national atmospheric deposition program: an overview, Atmospheric Environment, 34, 1661–1663, https://doi.org/10.1016/S1352-2310(99)00425-2, 2000.

Lamb, D. and Comrie, L.: Comparability and precision of MAP3S and NADP/NTN precipitation 845 chemistry data at an acidic site in eastern North America, Atmospheric Environment. Part A. General Topics, 27, 1993–2008, https://doi.org/10.1016/0960-1686(93)90273-2, 1993.

Lamsal, L. N., Martin, R. V., Padmanabhan, A., van Donkelaar, A., Zhang, Q., Sioris, C. E., Chance, K., Kurosu, T. P., and Newchurch, M. J.: Application of satellite observations for timely updates to global

anthropogenic NO $_x$ emission inventories: UPDATING NO $_x$ EMISSION INVENTORIES, Geophys. Res. Lett., 38, n/a-n/a, https://doi.org/10.1029/2010GL046476, 2011.

Laughner, J. L. and Cohen, R. C.: Direct observation of changing NO $_x$ lifetime in North American cities, Science, 366, 723–727, https://doi.org/10.1126/science.aax6832, 2019.

Li, Y., Schichtel, B. A., Walker, J. T., Schwede, D. B., Chen, X., Lehmann, C. M. B., Puchalski, M. A., Gay, D. A., and Collett, J. L.: Increasing importance of deposition of reduced nitrogen in the United States, Proc Natl Acad Sci USA, 113, 5874–5879, https://doi.org/10.1073/pnas.1525736113, 2016.

Liu, F., Beirle, S., Zhang, Q., Dörner, S., He, K., and Wagner, T.: NO$_x$ lifetimes and emissions of cities and power plants in polluted background estimated by satellite observations, Atmos. Chem. Phys., 16, 5283–5298, https://doi.org/10.5194/acp-16-5283-2016, 2016.

Liu, P., Kaplan, J. O., Mickley, L. J., Li, Y., Chellman, N. J., Arienzo, M. M., Kodros, J. K., Pierce, J. R., Sigl, M., Freitag, J., Mulvaney, R., Curran, M. A. J., and McConnell, J. R.: Improved estimates of preindustrial biomass burning reduce the magnitude of aerosol climate forcing in the Southern Hemisphere, Sci. Adv., 7, eabc1379, https://doi.org/10.1126/sciadv.abc1379, 2021.

Mao, J., Zhao, T., Keller, C. A., Wang, X., McFarland, P. J., Jenkins, J. M., and Brune, W. H.: Global Impact of Lightning-Produced Oxidants, Geophys Res Lett, 48, https://doi.org/10.1029/2021GL095740, 2021.

Martin, R. V.: An improved retrieval of tropospheric nitrogen dioxide from GOME, J. Geophys. Res., 107, 4437, https://doi.org/10.1029/2001JD001027, 2002.

Martin, R. V., Sauvage, B., Folkins, I., Sioris, C. E., Boone, C., Bernath, P., and Ziemke, J.: Space-based constraints on the production of nitric oxide by lightning, J. Geophys. Res., 112, 2006JD007831, https://doi.org/10.1029/2006JD007831, 2007.

McDonald, B. C., Gentner, D. R., Goldstein, A. H., and Harley, R. A.: Long-Term Trends in Motor Vehicle Emissions in U.S. Urban Areas, Environ. Sci. Technol., 47, 10022–10031, https://doi.org/10.1021/es401034z, 2013.

McDonald, B. C., McKeen, S. A., Cui, Y. Y., Ahmadov, R., Kim, S.-W., Frost, G. J., Pollack, I. B., Peischl, J., Ryerson, T. B., Holloway, J. S., Graus, M., Warneke, C., Gilman, J. B., de Gouw, J. A., Kaiser, J., Keutsch, F. N., Hanisco, T. F., Wolfe, G. M., and Trainer, M.: Modeling Ozone in the Eastern U.S. using a Fuel-Based Mobile Source Emissions Inventory, Environ. Sci. Technol., 52, 7360–7370, https://doi.org/10.1021/acs.est.8b00778, 2018.

McDuffie, E. E., Smith, S. J., O'Rourke, P., Tibrewal, K., Venkataraman, C., Marais, E. A., Zheng, B., Crippa, M., Brauer, M., and Martin, R. V.: A global anthropogenic emission inventory of atmospheric

pollutants from sector- and fuel-specific sources (1970–2017): an application of the Community Emissions Data System (CEDS), Earth Syst. Sci. Data, 12, 3413–3442, https://doi.org/10.5194/essd-12-3413-2020, 2020.

885 Meyers, T. P., Finkelstein, P., Clarke, J., Ellestad, T. G., and Sims, P. F.: A multilayer model for inferring dry deposition using standard meteorological measurements, J. Geophys. Res., 103, 22645–22661, https://doi.org/10.1029/98JD01564, 1998.

Miyazaki, K., Eskes, H., Sudo, K., Boersma, K. F., Bowman, K., and Kanaya, Y.: Decadal changes in global surface NO$_x$ emissions from multi-constituent
890 satellite data assimilation, Atmos. Chem. Phys., 17, 807–837, https://doi.org/10.5194/acp-17-807-2017, 2017.

Monks, P. S., Granier, C., Fuzzi, S., Stohl, A., Williams, M. L., Akimoto, H., Amann, M., Baklanov, A., Baltensperger, U., Bey, I., Blake, N., Blake, R. S., Carslaw, K., Cooper, O. R., Dentener, F., Fowler, D., Fragkou, E., Frost, G. J., Generoso, S., Ginoux, P., Grewe, V., Guenther, A., Hansson, H. C., Henne, S.,
895 Hjorth, J., Hofzumahaus, A., Huntrieser, H., Isaksen, I. S. A., Jenkin, M. E., Kaiser, J., Kanakidou, M., Klimont, Z., Kulmala, M., Laj, P., Lawrence, M. G., Lee, J. D., Liousse, C., Maione, M., McFiggans, G., Metzger, A., Mieville, A., Moussiopoulos, N., Orlando, J. J., O'Dowd, C. D., Palmer, P. I., Parrish, D. D., Petzold, A., Platt, U., Pöschl, U., Prévôt, A. S. H., Reeves, C. E., Reimann, S., Rudich, Y., Sellegri, K., Steinbrecher, R., Simpson, D., ten Brink, H., Theloke, J., van der Werf, G. R., Vautard, R., Vestreng,
900 V., Vlachokostas, Ch., and von Glasow, R.: Atmospheric composition change – global and regional air quality, Atmospheric Environment, 43, 5268–5350, https://doi.org/10.1016/j.atmosenv.2009.08.021, 2009.

Monks, P. S., Archibald, A. T., Colette, A., Cooper, O., Coyle, M., Derwent, R., Fowler, D., Granier, C., Law, K. S., Mills, G. E., Stevenson, D. S., Tarasova, O., Thouret, V., von Schneidemesser, E.,
905 Sommariva, R., Wild, O., and Williams, M. L.: Tropospheric ozone and its precursors from the urban to the global scale from air quality to short-lived climate forcer, Atmos. Chem. Phys., 15, 8889–8973, https://doi.org/10.5194/acp-15-8889-2015, 2015.

Murray, L. T.: Lightning NO x and Impacts on Air Quality, Curr Pollution Rep, 2, 115–133, https://doi.org/10.1007/s40726-016-0031-7, 2016.

910 Murray, L. T., Jacob, D. J., Logan, J. A., Hudman, R. C., and Koshak, W. J.: Optimized regional and interannual variability of lightning in a global chemical transport model constrained by LIS/OTD satellite data: IAV OF LIGHTNING CONSTRAINED BY LIS/OTD, J. Geophys. Res., 117, https://doi.org/10.1029/2012JD017934, 2012.

Murray, L. T., Logan, J. A., and Jacob, D. J.: Interannual variability in tropical tropospheric ozone and
915 OH: The role of lightning: IAV IN OZONE AND OH-ROLE OF LIGHTNING, J. Geophys. Res. Atmos., 118, 11,468-11,480, https://doi.org/10.1002/jgrd.50857, 2013.

Murray, L. T., Leibensperger, E. M., Orbe, C., Mickley, L. J., and Sulprizio, M.: GCAP 2.0: a global 3-D chemical-transport model framework for past, present, and future climate scenarios, Geosci. Model Dev., 14, 5789–5823, https://doi.org/10.5194/gmd-14-5789-2021, 2021.

920 Nilles, M. A., Gordon, J. D., and Schroder, L. J.: The precision of wet atmospheric deposition data from national atmospheric deposition program/national trends network sites determined with collocated samplers, Atmospheric Environment, 28, 1121–1128, https://doi.org/10.1016/1352-2310(94)90289-5, 1994.

Oner, E. and Kaynak, B.: Evaluation of NOx emissions for Turkey using satellite and ground-based 925 observations, Atmospheric Pollution Research, 7, 419–430, https://doi.org/10.1016/j.apr.2015.10.017, 2016.

Parrish, D. D.: Critical evaluation of US on-road vehicle emission inventories, Atmospheric Environment, 40, 2288–2300, https://doi.org/10.1016/j.atmosenv.2005.11.033, 2006.

Paulot, F., Jacob, D. J., Pinder, R. W., Bash, J. O., Travis, K., and Henze, D. K.: Ammonia emissions in 930 the United States, European Union, and China derived by high-resolution inversion of ammonium wet deposition data: Interpretation with a new agricultural emissions inventory (MASAGE_NH3), J. Geophys. Res. Atmos., 119, 4343–4364, https://doi.org/10.1002/2013JD021130, 2014.

Peischl, J., Ryerson, T. B., Holloway, J. S., Parrish, D. D., Trainer, M., Frost, G. J., Aikin, K. C., Brown, S. S., Dubé, W. P., Stark, H., and Fehsenfeld, F. C.: A top-down analysis of emissions from selected 935 Texas power plants during TexAQS 2000 and 2006, J. Geophys. Res., 115, D16303, https://doi.org/10.1029/2009JD013527, 2010.

Pope, C. A., Turner, M. C., Burnett, R. T., Jerrett, M., Gapstur, S. M., Diver, W. R., Krewski, D., and Brook, R. D.: Relationships Between Fine Particulate Air Pollution, Cardiometabolic Disorders, and Cardiovascular Mortality, Circulation Research, 116, 108–115, 940 https://doi.org/10.1161/CIRCRESAHA.116.305060, 2015.

Qu, Z., Jacob, D. J., Silvern, R. F., Shah, V., Campbell, P. C., Valin, L. C., and Murray, L. T.: US COVID-19 Shutdown Demonstrates Importance of Background NO_2 in Inferring NO_x Emissions From Satellite NO_2 Observations, Geophys Res Lett, 48, https://doi.org/10.1029/2021GL092783, 2021.

R Core Team: R: A language and environment for statistical computing., R Foundation for Statistical 945 Computing, Vienna, Austria, 2013.

Rienecker, M. M., Suarez, M. J., Gelaro, R., Todling, R., Bacmeister, J., Liu, E., Bosilovich, M. G., Schubert, S. D., Takacs, L., Kim, G.-K., Bloom, S., Chen, J., Collins, D., Conaty, A., da Silva, A., Gu, W., Joiner, J., Koster, R. D., Lucchesi, R., Molod, A., Owens, T., Pawson, S., Pegion, P., Redder, C. R., Reichle, R., Robertson, F. R., Ruddick, A. G., Sienkiewicz, M., and Woollen, J.: MERRA: NASA's

Modern-Era Retrospective Analysis for Research and Applications, Journal of Climate, 24, 3624–3648, https://doi.org/10.1175/JCLI-D-11-00015.1, 2011.

Rossi, R., Ceccato, R., and Gastaldi, M.: Effect of Road Traffic on Air Pollution. Experimental Evidence from COVID-19 Lockdown, Sustainability, 12, 8984, https://doi.org/10.3390/su12218984, 2020.

Salmon, O. E., Shepson, P. B., Ren, X., He, H., Hall, D. L., Dickerson, R. R., Stirm, B. H., Brown, S. S., Fibiger, D. L., McDuffie, E. E., Campos, T. L., Gurney, K. R., and Thornton, J. A.: Top-Down Estimates of NOx and CO Emissions From Washington, D.C.-Baltimore During the WINTER Campaign, J. Geophys. Res. Atmos., 123, 7705–7724, https://doi.org/10.1029/2018JD028539, 2018.

Schultz, M. G., Schröder, S., Lyapina, O., Cooper, O. R., Galbally, I., Petropavlovskikh, I., von Schneidemesser, E., Tanimoto, H., Elshorbany, Y., Naja, M., Seguel, R. J., Dauert, U., Eckhardt, P., Feigenspan, S., Fiebig, M., Hjellbrekke, A.-G., Hong, Y.-D., Kjeld, P. C., Koide, H., Lear, G., Tarasick, D., Ueno, M., Wallasch, M., Baumgardner, D., Chuang, M.-T., Gillett, R., Lee, M., Molloy, S., Moolla, R., Wang, T., Sharps, K., Adame, J. A., Ancellet, G., Apadula, F., Artaxo, P., Barlasina, M. E., Bogucka, M., Bonasoni, P., Chang, L., Colomb, A., Cuevas-Agulló, E., Cupeiro, M., Degorska, A., Ding, A., Fröhlich, M., Frolova, M., Gadhavi, H., Gheusi, F., Gilge, S., Gonzalez, M. Y., Gros, V., Hamad, S. H., Helmig, D., Henriques, D., Hermansen, O., Holla, R., Hueber, J., Im, U., Jaffe, D. A., Komala, N., Kubistin, D., Lam, K.-S., Laurila, T., Lee, H., Levy, I., Mazzoleni, C., Mazzoleni, L. R., McClure-Begley, A., Mohamad, M., Murovec, M., Navarro-Comas, M., Nicodim, F., Parrish, D., Read, K. A., Reid, N., Ries, L., Saxena, P., Schwab, J. J., Scorgie, Y., Senik, I., Simmonds, P., Sinha, V., Skorokhod, A. I., Spain, G., Spangl, W., Spoor, R., Springston, S. R., Steer, K., Steinbacher, M., Suharguniyawan, E., Torre, P., Trickl, T., Weili, L., Weller, R., Xiaobin, X., Xue, L., and Zhiqiang, M.: Tropospheric Ozone Assessment Report: Database and metrics data of global surface ozone observations, Elementa: Science of the Anthropocene, 5, 58, https://doi.org/10.1525/elementa.244, 2017.

Schwede, D. B. and Lear, G. G.: A novel hybrid approach for estimating total deposition in the United States, Atmospheric Environment, 92, 207–220, https://doi.org/10.1016/j.atmosenv.2014.04.008, 2014.

Shah, V., Jacob, D. J., Li, K., Silvern, R. F., Zhai, S., Liu, M., Lin, J., and Zhang, Q.: Effect of changing NO_x lifetime on the seasonality and long-term trends of satellite-observed tropospheric NO_2 columns over China, Gases/Atmospheric Modelling/Troposphere/Chemistry (chemical composition and reactions), https://doi.org/10.5194/acp-2019-670, 2019.

Shah, V., Jacob, D. J., Dang, R., Lamsal, L. N., Strode, S. A., Steenrod, S. D., Boersma, K. F., Eastham, S. D., Fritz, T. M., Thompson, C., Peischl, J., Bourgeois, I., Pollack, I. B., Nault, B. A., Cohen, R. C., Campuzano-Jost, P., Jimenez, J. L., Andersen, S. T., Carpenter, L. J., Sherwen, T., and Evans, M. J.: Nitrogen oxides in the free troposphere: Implications for tropospheric oxidants and the interpretation of satellite NO_2 measurements, Gases/Atmospheric Modelling/Troposphere/Chemistry (chemical composition and reactions), https://doi.org/10.5194/egusphere-2022-656, 2022.

Sickles II, J. E. and Shadwick, D. S.: Air quality and atmospheric deposition in the eastern US: 20 years of change, Atmos. Chem. Phys., 15, 173–197, https://doi.org/10.5194/acp-15-173-2015, 2015.

990 Silvern, R. F., Jacob, D. J., Mickley, L. J., Sulprizio, M. P., Travis, K. R., Marais, E. A., Cohen, R. C., Laughner, J. L., Choi, S., Joiner, J., and Lamsal, L. N.: Using satellite observations of tropospheric NO<sub>2</sub> columns to infer long-term trends in US NO<sub><i>x</i></sub> emissions: the importance of accounting for the free tropospheric NO<sub>2</sub> background, Atmos. Chem. Phys., 19, 8863–8878, https://doi.org/10.5194/acp-19-8863-2019, 2019.

995 Singh, A. and Agrawal, M.: Acid rain and its ecological consequences, Journal of Environmental Biology, 29, 15–24, 2008.

Souri, A. H., Choi, Y., Jeon, W., Li, X., Pan, S., Diao, L., and Westenbarger, D. A.: Constraining NOx emissions using satellite NO2 measurements during 2013 DISCOVER-AQ Texas campaign, Atmospheric Environment, 131, 371–381, https://doi.org/10.1016/j.atmosenv.2016.02.020, 2016.

1000 Stavrakou, T., Müller, J.-F., Boersma, K. F., van der A, R. J., Kurokawa, J., Ohara, T., and Zhang, Q.: Key chemical NO<sub>x</sub> sink uncertainties and how they influence top-down emissions of nitrogen oxides, Atmos. Chem. Phys., 13, 9057–9082, https://doi.org/10.5194/acp-13-9057-2013, 2013.

Sterling, C. W., Johnson, B. J., Oltmans, S. J., Smit, H. G. J., Jordan, A. F., Cullis, P. D., Hall, E. G., 1005 Thompson, A. M., and Witte, J. C.: Homogenizing and estimating the uncertainty in NOAA's long-term vertical ozone profile records measured with the electrochemical concentration cell ozonesonde, Atmos. Meas. Tech., 11, 3661–3687, https://doi.org/10.5194/amt-11-3661-2018, 2018.

Szymankiewicz, K., Kaminski, J. W., and Struzewska, J.: Application of Satellite Observations and Air Quality Modelling to Validation of NOx Anthropogenic EMEP Emissions Inventory over Central Europe, 1010 Atmosphere, 12, 1465, https://doi.org/10.3390/atmos12111465, 2021.

Takenoue, Y., Kaneko, T., miyamae, T., Mori, M., and Yokota, S.: Influence of outdoor NO 2 exposure on asthma in childhood: Meta-analysis: Influence of NO 2 exposure in childhood, Pediatr Int, 54, 762–769, https://doi.org/10.1111/j.1442-200X.2012.03674.x, 2012.

Tarasick, D. W., Davies, J., Smit, H. G. J., and Oltmans, S. J.: A re-evaluated Canadian ozonesonde 1015 record: measurements of the vertical distribution of ozone over Canada from 1966 to 2013, Atmos. Meas. Tech., 9, 195–214, https://doi.org/10.5194/amt-9-195-2016, 2016.

Tørseth, K., Aas, W., Breivik, K., Fjæraa, A. M., Fiebig, M., Hjellbrekke, A. G., Lund Myhre, C., Solberg, S., and Yttri, K. E.: Introduction to the European Monitoring and Evaluation Programme (EMEP) and observed atmospheric composition change during 1972–2009, Atmos. Chem. Phys., 12, 5447–5481, 1020 https://doi.org/10.5194/acp-12-5447-2012, 2012.

Travis, K. R., Jacob, D. J., Fisher, J. A., Kim, P. S., Marais, E. A., Zhu, L., Yu, K., Miller, C. C., Yantosca, R. M., Sulprizio, M. P., Thompson, A. M., Wennberg, P. O., Crounse, J. D., St. Clair, J. M., Cohen, R. C., Laughner, J. L., Dibb, J. E., Hall, S. R., Ullmann, K., Wolfe, G. M., Pollack, I. B., Peischl, J., Neuman, J. A., and Zhou, X.: Why do models overestimate surface ozone in the Southeast United States?, Atmospheric Chemistry and Physics, 16, 13561–13577, https://doi.org/10.5194/acp-16-13561-2016, 2016.

Turner, M. C., Krewski, D., Pope, C. A., Chen, Y., Gapstur, S. M., and Thun, M. J.: Long-term Ambient Fine Particulate Matter Air Pollution and Lung Cancer in a Large Cohort of Never-Smokers, American Journal of Respiratory and Critical Care Medicine, 184, 1374–1381, https://doi.org/10.1164/rccm.201106-1011OC, 2011.

Van Malderen, R., Allaart, M. A. F., De Backer, H., Smit, H. G. J., and De Muer, D.: On instrumental errors and related correction strategies of ozonesondes: possible effect on calculated ozone trends for the nearby sites Uccle and De Bilt, Atmos. Meas. Tech., 9, 3793–3816, https://doi.org/10.5194/amt-9-3793-2016, 2016.

Vinken, G. C. M., Boersma, K. F., van Donkelaar, A., and Zhang, L.: Constraints on ship NO_x emissions in Europe using GEOS-Chem and OMI satellite NO_2 observations, Atmos. Chem. Phys., 14, 1353–1369, https://doi.org/10.5194/acp-14-1353-2014, 2014.

Wang, X., Jacob, D. J., Eastham, S. D., Sulprizio, M. P., Zhu, L., Chen, Q., Alexander, B., Sherwen, T., Evans, M. J., Lee, B. H., Haskins, J. D., Lopez-Hilfiker, F. D., Thornton, J. A., Huey, G. L., and Liao, H.: The role of chlorine in global tropospheric chemistry, Atmos. Chem. Phys., 19, 3981–4003, https://doi.org/10.5194/acp-19-3981-2019, 2019.

Wang, X., Jacob, D. J., Downs, W., Zhai, S., Zhu, L., Shah, V., Holmes, C. D., Sherwen, T., Alexander, B., Evans, M. J., Eastham, S. D., Neuman, J. A., Veres, P. R., Koenig, T. K., Volkamer, R., Huey, L. G., Bannan, T. J., Percival, C. J., Lee, B. H., and Thornton, J. A.: Global tropospheric halogen (Cl, Br, I) chemistry and its impact on oxidants, Atmos. Chem. Phys., 21, 13973–13996, https://doi.org/10.5194/acp-21-13973-2021, 2021.

Witte, J. C., Thompson, A. M., Smit, H. G. J., Vömel, H., Posny, F., and Stübi, R.: First Reprocessing of Southern Hemisphere ADditional OZonesondes Profile Records: 3. Uncertainty in Ozone Profile and Total Column, JGR Atmospheres, 123, 3243–3268, https://doi.org/10.1002/2017JD027791, 2018.

Zhang, L., Jacob, D. J., Knipping, E. M., Kumar, N., Munger, J. W., Carouge, C. C., van Donkelaar, A., Wang, Y. X., and Chen, D.: Nitrogen deposition to the United States: distribution, sources, and processes, Atmos. Chem. Phys., 12, 4539–4554, https://doi.org/10.5194/acp-12-4539-2012, 2012.